Developing and exploiting optogenetic feedback control in mesoscale neuroscience

Thesis Proposal
Biomedical Engineering PhD Program
Georgia Institute of Technology and Emory University

Kyle Johnsen

1/1/23

As the importance of causal inference becomes increasingly recognized in neuroscience, the need for technology enabling precise manipulation of neural variables becomes apparent. Feedback control is an important class of such manipulations for its ability to increase inference power by reducing response variability. Widely used throughout the engineering disciplines, it has had a significant impact through a variety of techniques (e.g., voltage clamp, dynamic clamp) on cellular neuroscience. However, feedback control has yet to be widely applied at the mesoscale/circuit level despite recent improvements in interfacing technology, such as optogenetics. Challenges to adoption include the complexity of implementing fast closed-loop experiments, the need to adapt the mature methods of control theory to the idiosyncratic constraints of systems neuroscience experiments, and the lack of established technical guidelines for applying feedback control to address complex scientific questions.

In this work I propose to begin to address these challenges in three aims. In Aim 1, I develop a simulation framework for easily prototyping closed-loop optogenetic control (CLOC) experiments *in silico*, thus allowing neuroscientists to test and iterate on experimental designs without the costs of in-vivo experiments or up-front investments in compatible hardware-software systems. In Aim 2, I will translate sophisticated model-based feedback control algorithms to the realistic experimental setting of multi-input CLOC—the simultaneous use of multiple light sources, which includes the bidirectional case of both excitatory and inhibitory opsins. I will demonstrate some advantages of multi-input CLOC and how it is not well accommodated by the algorithms previously demonstrated. Finally, in Aim 3, I will explore how recording, stimulation, and control requirements vary in an example application of CLOC—controlling the latent dynamics of simulated neural population activity and assessing their causal relationship with behavior. I will model this population activity with recurrent spiking neural networks trained using state-of-the-art, biologically plausible methods, with differing degrees of brain-like architecture and task complexity. This work will thus provide the systems neuroscience community with a more accessible entry point for CLOC, more powerful algorithms for leveraging multi-input control, and a point of reference for designing CLOC experiments capable of answering complex scientific questions.

Front Matter

Thesis committee

Nabil Imam	Georgia Institute of Technology Computational Science and Engineering
Chethan Pandarinath	Emory University & Georgia Institute of Technology Biomedical Engineering
Christopher Rozell (advisor)	Georgia Institute of Technology Electrical and Computer Engineering
Garrett Stanley	Georgia Institute of Technology & Emory University Biomedical Engineering
Patricio Vela	Georgia Institute of Technology Electrical and Computer Engineering

Table of contents

1 Specific Aims

1.1 Rationale

As the importance of causal inference becomes increasingly recognized in neuroscience, the need for technology enabling precise manipulation of neural variables becomes apparent. Feedback control is an important class of such manipulations for its ability to increase inference power by reducing response variability. Widely used throughout the engineering disciplines, it has had a significant impact through a variety of techniques (e.g., voltage clamp, dynamic clamp) on cellular neuroscience. However, feedback control also has great potential at the mesoscale/systems level, potentially enabling researchers to *unambiguously infer the downstream effects of circuit/population-level neural activity.*

For a number of reasons, though, *this potential has not been widely realized.* The main challenges to wider adoption do not appear to lie with available technology, as the computational power and stimulation/recording requirements of feedback control are met by the ever-improving tools already available to neuroscientists, such as optogenetics and large-scale neural recording. I posit that the main challenges to adoption rather include the **complexity of implementing** fast closed-loop experiments, the need to **adapt the mature methods of control theory** to the idiosyncratic constraints of systems neuroscience experiments, and the **lack of established technical guidelines** for applying feedback control to address complex scientific questions. **The proposed work aims to begin to address these challenges, and thus strengthen the set of causal tools available to probe neural systems.**

1.2 Aim 1: A CLOC experiment simulation testbed

One significant obstacle to closed-loop optogenetic control (CLOC) experiments is the cost of acquiring and configuring compatible hardware-software systems. Moreover, the maintenance of animals or cell cultures inherent in lab experiments can slow the pace of developing novel techniques. In Aim 1, I attempt to address these obstacles by developing a simulation framework for easily prototyping CLOC experiments *in silico*, thus enabling faster, cheaper CLOC experiment design and method development. We demonstrate the software's utility in different virtual experiments and provide it to the public as open-source software with thorough documentation.

1.3 Aim 2: Multi-input CLOC

Multi-input CLOC—the simultaneous use of multiple light sources—is necessary for precise manipulation of neural systems, especially when bidirectional actuation (both excitatory and inhibitory opsins) is needed to maintain naturalistic activity levels. However, the basic control theory methods previously used in conjuction with CLOC do not take actuator constraints into account and are thus inadequate for multi-actuator (i.e., multi-light source) problems. The field of control theory provides elegant, powerful solutions to this class of problems, but applying them requires interdisciplinary expertise. In this aim I will translate more sophisticated model-based feedback control algorithms to the multi-input CLOC setting and demonstrate the advantages both of bidirectional actuation and these algorithmic improvements.

1.4 Aim 3: Using CLOC to manipulate latent neural dynamics

To our knowledge, CLOC has yet to be applied in answering complex systems neuroscience questions. In this aim, to pave the way for future *in-vivo* experiments that accomplish this, I propose to develop technical and conceptual guidelines as I control the latent dynamics of simulated neural populations. First, I will produce these virtual models by training recurrent spiking neural networks with state-of-the-art, biologically plausible methods—each differing in their degrees of brain-like architecture and training procedure complexity. I will then use the simulation testbed of Aim 1 to explore how recording, stimulation, and control requirements vary with the complexity and size of the system—thus giving researchers some idea of the relative importance of each factor of CLOC. Finally, I will demonstrate the conceptual utility of CLOC by quantitatively assessing the causal relationship between these latent dynamics and "behavior" (model output).

2 Background

2.1 Closed-loop control in neuroscience

Mesoscale neuroscience—on the level of populations of neurons, rather than the whole brain or individual cells—is currently undergoing a revolution fueled by advances in neural manipulation (Adesnik and Abdeladim, 2021; Eriksson et al., 2022; Faini et al., 2021; Fenno et al., 2011; Roth, 2016; Sridharan et al., 2022; Vierock et al., 2021; Wiegert et al., 2017) and measurement (Göbel and Helmchen, 2007; Gutruf and Rogers, 2018; Kazemipour et al., 2019; Knöpfel and Song, 2019; Siegle et al., 2017; Steinmetz et al., 2021; Svoboda and Yasuda, 2006; Wu et al., 2020) technologies as well as data analysis methods (Berman et al., 2014; Maaten and Hinton, 2008; Mathis et al., 2018; Sani et al., 2021a; Schneider et al., 2022; Sporns, 2018). These have yielded unprecedented datasets (Juavinett et al., 2019; Scheffer et al., 2020) and insights into network activity and plasticity (Avitan and Stringer, 2022; Cowley et al., 2020; Jazayeri and Ostojic, 2021; Oby et al., 2019; Yang et al., 2021), as well as novel experimental paradigms such as direct closed-loop control of neural activity (Bolus et al., 2021, 2018; Dutta et al., 2019; Grosenick et al., 2015; Krook-Magnuson et al., 2013; Kumar et al., 2013; Newman et al., 2015; Potter et al., 2014; Witt et al., 2013; Zhang et al., 2018). This closed-loop control of neural activity offers exciting prospects of intervention in processes that are too fast or unpredictable to control manually or with pre-defined stimulation, such as sensory information processing, motor planning, and oscillatory activity. Unlike other forms of closed-loop control using environmental/stimulus input (Tafazoli et al., 2020), behavioral output (Srinivasan et al., 2018) or neurofeedback training (Eriksson et al., 2022; Prsa et al., 2017), the direct control of neural activity itself can unambiguously reveal the downstream effects of that activity.

2.1.1 Types of closed-loop control

Closed-loop control of neural activity can be implemented in an event-triggered sense (Dutta et al., 2019; Krook-Magnuson et al., 2013; Witt et al., 2013)—enabling the experimenter to respond to discrete events of interest, such as the arrival of a traveling wave (Davis et al., 2020) or sharp wave ripple (Buzsáki, 2015)—or in a feedback sense (Bolus et al., 2021, 2018; Newman et al., 2015; Zhang et al., 2018), driving the system towards a target or along a trajectory. The latter has multiple advantages over open-loop control (delivery of a pre-defined stimulus): by rejecting exogenous inputs, noise, and disturbances, it reduces variability across time and across trials, allowing for finer-scale inference. Additionally, it can compensate for

model mismatch, allowing it to succeed where open-loop control based on imperfect models is bound to miss the mark. Moreover, whereas traditional perturbation methods often include lesioning (Vaidya et al., 2019), unnatural silencing, or extreme stimulation, feedback control poses a more naturalistic alternative, increasing generalizability. Clamping the activity of a population of neurons to their baseline, for example, effectively shuts down information flow from those neurons without departing from constitutive firing rates.

2.2 Various scales and tools for closed-loop control

Closed-loop control of neural activity can be performed at multiple scales and with different sets of tools. At the smallest, sub-neuron scale, dynamic clamping has yielded decades of fruitful research in the forms of tools such as the voltage clamp (Hodgkin et al., 1952) and dynamic clamp (Hodgkin and Huxley, 1952; Prinz et al., 2004; Sharp et al., 1993), controlling electrical properties of small patches of membrane. The frontiers of this small-scale neuroscience often involve scaling up to many neurons and scaling down to subcellular structures such as dendrites, but multi-electrode, *in-vivo*, intracellular recording methods are challenging (Alegria et al., 2020; Davie et al., 2006; Engel, 2016; Peng et al., 2019; Wang et al., 2015). Optical tools—e.g., optogenetics and fluorescence microscopy—can circumvent the difficulties of working with electrodes at such small scales, but an optical approach is not yet feasible for this purpose. The obstacles lie mainly in recording technology: the kinetics of both voltage indicators (Wu et al., 2020) and intracellular calcium (Inoue, 2021) are too slow to capture phenomena faster than a typical action potential.

By contrast, the current state of technology is ripe for innovating closed-loop control methods at larger scales of neural activity, from single neurons to populations and circuits. Several promising combinations of recording and stimulation modalities are possible and still relatively novel: electrode recording with optogenetic stimulation Newman et al. (2015), fluorescence microscopy with electrical stimulation (Wu et al., 2020), fluorescence microscopy with photostimulation (all-optical control) (Emiliani et al., 2015; Flytzanis et al., 2014; Hochbaum et al., 2014; Kishi et al., 2022; Zhang et al., 2018), and fMRI with optionally transcranial (S. Chen et al., 2018; Lin et al., 2013) photostimulation. Each of these tool combinations has pros and cons in terms of spatial and temporal resolution, crosstalk (Packer et al., 2013), and degrees of freedom.

A natural starting point for many neuroscientists is the first of these tool sets—electrode recording combined with optogenetics—since the two methods are so widely used, interfere little with each other (as long as metal electrodes are not directly illuminated (Cardin et al., 2010; Packer et al., 2013)), and allow for genetically targeted stimulation. I will henceforth refer to this combination as CLOC, following the convention established by previous works (Bolus et al., 2021, 2018).

2.3 Previous work

The proposed work builds on the work my lab and collaborators have done previously in implementing CLOC feedback control. Newman et al. (2015) demonstrated bidirectional CLOC for fixed firing and slowly varying rate targets and using a model-free proportional-integral (PI) control scheme *in silico* (Figure 2.1a), as well as unidirectional integral control in the anesthetized rat. Bolus et al. (2018) used PI control again, but developed a more principled approach to set estimation and control parameters and tracked dynamic firing rate trajectories down to a ~100-ms timescale (Figure 2.1b). Bolus et al. later employed more sophisticated and scalable optimal feedback control methods which are more robust to disturbances—important especially in awake animal experiments, where dynamic brain state changes contribute to high per-trial variability (Figure 2.1c).

2.4 Potential applications in mesoscale neuroscience

Seeing that a suitable technological foundation for feedback control of neural activity has already been laid with CLOC, I turn now to a discussion of several exciting areas where CLOC could further causal hypothesis testing. These deal with concrete questions of scientific interest, as opposed to the conceptual/technical advantages previously explained (Section 2.1). Neuroscientists often identify specific variables or phenomena to assess their role in a larger neural system, in search of interpretable components of brain activity. A natural application of CLOC is to control these variables and phenomena of interest directly to enable stronger inference of their relationship to downstream variables. Examples of these potential targets for control include the activity of different cell types (Joglekar et al., 2021; Lee et al., 2020; Martinez-Garcia et al., 2020; Mukamel and Ngai, 2019; Němec and Osten, 2020; Zeng, 2022); the type (Cole and Voytek, 2017; Cole and Voytek, 2019; Fabus et al., 2021), frequency (Saleem et al., 2017), amplitude (Saleem et al., 2017), spike coherence (Buffalo et al., 2011; Buschman et al., 2012) and interactions (Aru et al., 2015; Zhang et al., 2019) of different oscillatory patterns (Buzsáki and Draguhn, 2004); discrete phenomena such as bursts (Gerstner et al., 2014), sharp wave ripples (Buzsáki, 2015), oscillatory bursts (Akam and Kullmann, 2014; Karvat et al., 2020; Lundqvist et al., 2022; Lundqvist et al., 2016; Tal et al., 2020), traveling waves (Davis et al., 2020; Moldakarimov et al., 2018; Muller et al., 2018; Rule et al., 2018; Sato et al., 2012; Zhang et al., 2018), or sleep spindles (Fernandez and Lüthi, 2020); and latent states describing neural dynamics (Churchland et al., 2012; Cunningham and Yu, 2014; Gallego et al., 2017; Kaufman et al., 2014; Peixoto et al., 2021; Shenoy et al., 2013; Shenoy and Kao, 2021; Vyas et al., 2020), including those most relevant to behavior (Hurwitz et al., 2021; Sani et al., 2021a, 2021b).

While some of these targets lend themselves easily to CLOC, others require continued innovation in interfacing technology. Specifically, stimulation technologies have been much more limited in their degrees of freedom than modern recording technology (Göbel and Helmchen,

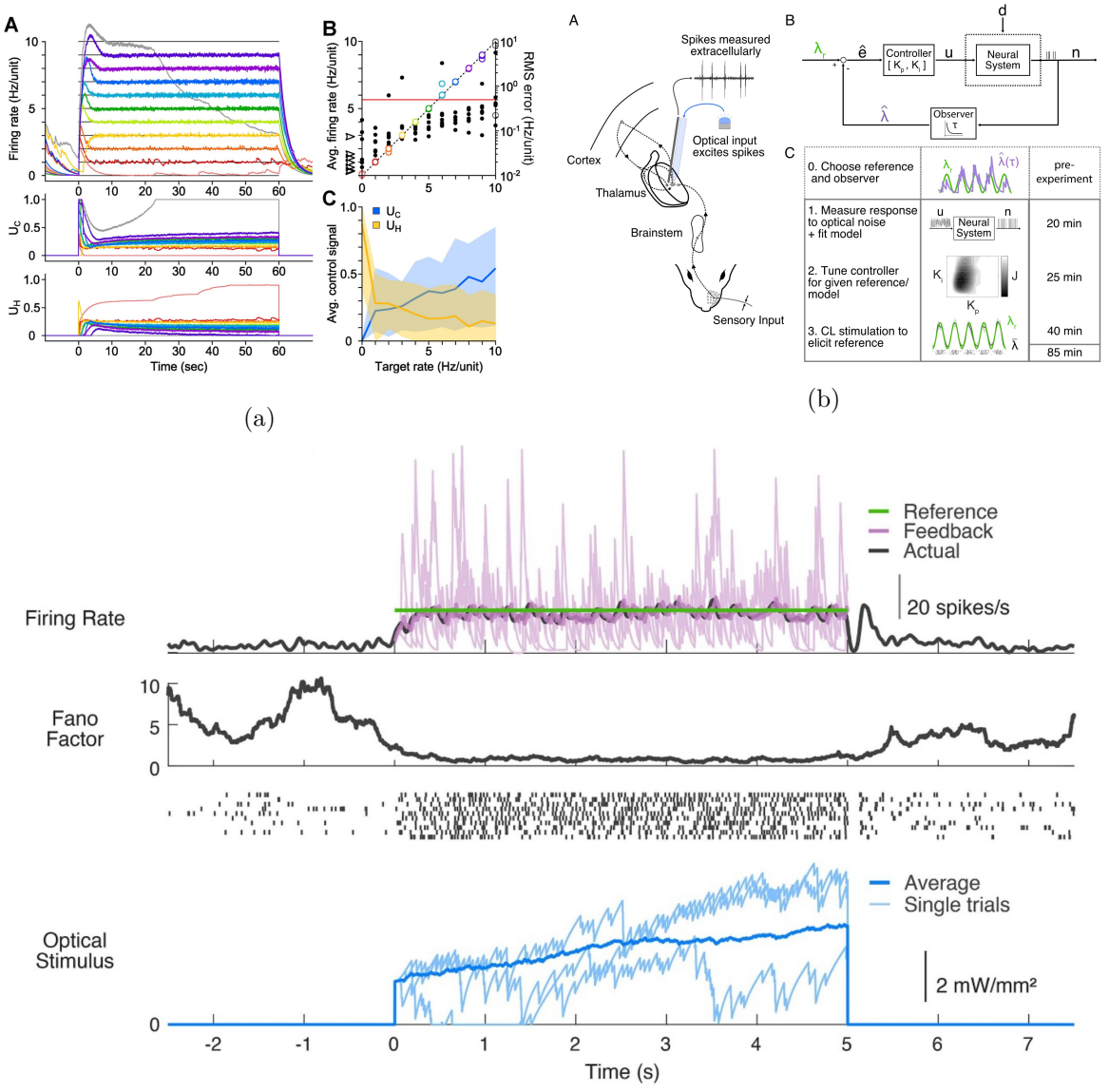

(a) (b) (c)

Figure 2.1: Previous CLOC experiments. (A) Figure 2 from Newman et al. (2015), demonstrating control clamping a cultured neuron to different firing rates. U_C refers to the control signal for channelrhodopsin2(H134R) ($ChR2_R$), parametrizing 470-nm light delivery. U_H likewise parametrizes 590-nm light delivery to activate enhanced halorhodopsin-3.0 (eNpHR3.0). (B) Figure 2 from Bolus et al. (2018), outlining an *in-vivo* experiment setup, a control diagram showing how optical input is determined from the firing rate estimated in real time, and a strategy for tuning the controller. (C) Figure 4b from Bolus et al. (2021), showing how CLOC clamps the firing rate of a single thalamic neuron in the awake mouse over multiple trials, reducing response variability (as measured by the Fano factor).

2007; Gutruf and Rogers, 2018; Kazemipour et al., 2019; Knöpfel and Song, 2019; Siegle et al., 2017; Steinmetz et al., 2021; Svoboda and Yasuda, 2006; Wu et al., 2020), and thus unlikely to sufficiently control what is observed. For this reason, the development of multi-channel micro-LED/optrode devices (Antolik et al., 2021; Dufour and Koninck, 2015; Eriksson et al., 2022; Jeon et al., 2021; Kathe et al., 2022; Kwon et al., 2015; Mao et al., 2021; Mao et al., 2019; McAlinden et al., 2019; Ohta et al., 2021; Wang et al., 2018; Welkenhuysen et al., 2016) and holographic optogenetic stimulation (I.-W. Chen et al., 2018; Packer et al., 2015; Ronzitti et al., 2017; Sridharan et al., 2022; Zhang et al., 2018) are of particular interest. Moreover, rigorous investigation of the importance of recording and stimulation capabilities relative to each other would be helpful in guiding technological development and experimental design.

In addition to controlling variables of interest, CLOC can serve a paradigm of decoupling variables. This could be in the context of a circuit, where clamping the activity of a given node decouples its activity from all inputs except for the controller. This functionally severs links in the circuit, aiding in circuit identification and in testing the function of different nodes and connections (**willats-clinc?**). Moreover, CLOC could be used in the more general sense of controlling for confounding variables. For example, one might want to manipulate the synchrony of a population without changing the mean firing rate, or vice-versa. Whereas the conventional open-loop stimulation approach might accomplish this through tedious titration of stimulation parameters (Nandy et al., 2019), the feedback control approach could simultaneously manipulate both variables as desired, requiring only a passable model of the system.

2.5 Innovation

Despite CLOC's great promise to be applied in these areas, it has not yet been widely applied in mesoscale neuroscience. As outlined in Section 1.1, I identify three main reasons for this, which I will begin to address. First, CLOC experiments are difficult and costly. I propose lowering the barrier to entry and the cost of experiment design and method development for CLOC experiments by creating a simulation framework, since **existing mesoscale neural network simulators do not contain the necessary ingredients for CLOC simulation**. Second, the algorithms previously used for CLOC are not well suited for actuation via multiple simultaneous light sources. I propose adapting more **powerful control theory methods** to enable multi-input CLOC, which to our knowledge **has not been done previously**. Third, technical and conceptual guidelines for the effective application of CLOC do not exist because **CLOC has not yet been applied to answer a complex scientific question**. I propose to model how this can be done by controlling latent neural dynamics *in silico*, exploring how technical requirements scale with model and experiment parameters and inferring a causal relationship between latent variables and model behavior.

3 Aim 1: A CLOC simulation testbed

3.1 Rationale

CLOC experiments are difficult and costly. This can be a barrier to entry for neuroscientists that find CLOC's advantages attractive. Their lab might lack the funds to invest in necessary hardware or the time to invest in adding high-performance signal processing loop to their experimental workflow. Or, they may possess the resources but do not want to spend them without some assurance that their proposed experiment would be fruitful. Finally, when the proposed experiment requires signal processing/control method development, iterating on designs *in-vivo* may be cumbersome, given the additional cost of animal care and training.

Taken together, these factors not only make CLOC experiments a significant investment for a researcher, but one laden with risk. Unknown properties of the system under study can make it hard to predict whether a proposed experiment (e.g., whether a given population of neurons can be controlled in a given way) is likely to succeed, and even more so when working with innovative methods with little precedent in the literature.

However, these costs and risks can be mitigated through in silico prototyping. Given a reliable model of the system of interest, one can simulate a proposed experiment, assessing the effectiveness of a given setup. Alternate models can be tested to assess robustness of the given method to unknown model properties, or a single method can be validated on a variety of models to determine its general applicability. This strategy not only allows for a researcher to evaluate and optimize methods before committing significant resources to them, but also accelerates the development cycle.

3.1.1 Innovation

For these reasons, I have developed Cleo: Closed Loop, Electrophysiology, and Optogenetics experiment simulation testbed. Unlike existing software, Cleo simultaneously provides a high-level interface to fast and flexible neural network simulations; easy, model-independent injection of electrode recording and optogenetic perturbations; and a real-time, closed-loop processing module capable of modeling communication and processing delays inherent in real experiments. I thus provide a "free trial" to researchers who are unsure if CLOC will serve their research agenda, as well as a low-cost environment to design experiments and develop methods, for those who are already committed to the technqiue.

3.2 Approach

3.2.1 Guiding principles

Two factors drove our choice of recording and stimulation models to integrate into Cleo. First, because a main purpose of Cleo is to enable prototyping of experiments, we focused on models at the level of the parameters an experimenter is able to alter. Because parameters such as electrode location, channel count and density, and optic fiber depth and size are all defined naturally in spatially extended models, Cleo's electrode and optogenetics modules require a "spatial" network model where relevant neurons must be assigned coordinates in space.

Second, we assumed that highly realistic models of individual neurons are not needed to capture most mesoscale-level phenomena. Accordingly, Cleo was developed with the intention of using point neurons models, rather than multi-compartment neuron models with realistic morphologies. Simulating simpler neuron models offers advantages of speed and intuitiveness, which are important in the context of prototyping an experiment. This decision had consequences in our software (Section 3.2.2) and LFP modeling (Section 3.2.3) decisions.

In addition to our modeling priorities, the goals of usability, flexibility, and extensibility guided our choices in software dependencies and infrastructure. Ease of use is important to make Cleo as accessible as possible, especially to researchers with primarily experimental backgrounds who may not have extensive experience with computational modeling. This usability goal also motivated Cleo's modular design, which allows users to add different recording or stimulation devices with little or no modification to the underlying network model, easing the burden of testing a variety of experimental configurations. Flexibility in the underlying simulator, in addition to enabling compatibility with a wide variety of models, is necessary for arbitrarily interacting with the simulation in a closed-loop fashion. Finally, extensibility is important for the testbed to remain relevant under changing needs in the future, allowing for new functionality to be easily added in a "plug-in," modular architecture.

3.2.2 Closed-loop simulation architecture

We chose Brian 2 (Stimberg et al., 2019) as the spiking neural network simulator to build Cleo around. Brian is a relatively new spiking neural network simulator written in Python with multiple advantages. It flexibly allows (and even requires) the user to define models mathematically rather than selecting from a pre-defined library of cell types and features, while maintaining the ease of a high-level interface. This keeps model and experiment details together and enables us to define arbitrary recording and stimulation models that easily interface with the simulation. Moreover, the Python programming language has the advantages of being open-source, intuitive to learn (Bogdanchikov et al., 2013), and widely used in computational neuroscience (Davison et al., 2009; Muller et al., 2015). Users do not need to use any other languages to use Brian. Brian is also relatively fast (especially since it is developed primarily for point neuron simulations), as shown in benchmarks (Stimberg et al., 2019).

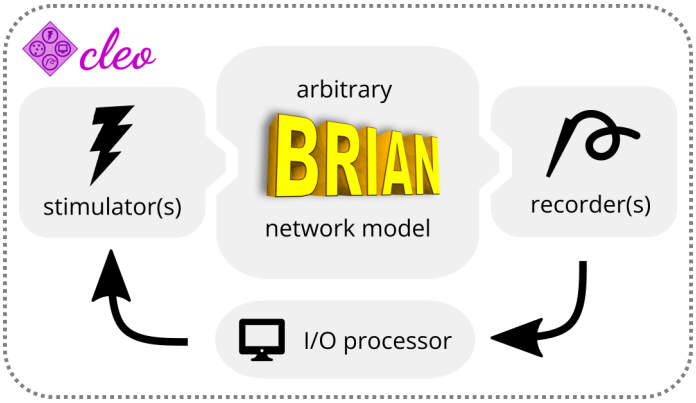

Figure 3.1: A conceptual diagram of Cleo's functionality. Cleo wraps a Brian network model, injects stimulation and recording devices, and interfaces with the network in real time through a simulated "I/O processor".

Cleo provides three modules—recording, stimulation, and closed-loop processing—for integration with an existing Brian model (see Figure 3.1). Cleo's functionality centers around a `CLSimulator` object that orchestrates the interactions between these three modules and the Brian simulation by injecting devices, running the simulation, and communicating with an `IOProcessor` object at each time step. The `IOProcessor` receives recorder measurements according to a specified sampling rate and returns any updates to stimulator devices.

In order to simulate the effects of latency in closed-loop control, Cleo provides a `LatencyIOProcessor` class capable of delivering control signals after some delay. It does this by storing the outputs calculated for every sample in a buffer along with the time they can be delivered to the network. For example, if a sample is taken at 20 ms and the user wishes to simulate a processing and communication latency of 3 ms, the control signal, along with the output time of 23 ms is stored in a buffer which the simulation checks at every timestep. As soon as the simulation clock reaches 23 ms, the control signal is taken from the buffer and applied to the stimulator devices. Because the user has arbitrary control over this latency, they can easily simulate probabilistic delays if, for example, they wish to assess the effect of the experimental platform stalling occasionally.

By default, `LatencyIOProcessor` samples on a fixed schedule and simulates processing samples in parallel—that is, the computation time for one sample does not affect that of others. Some alternatives are available, as illustrated in Figure 3.2.

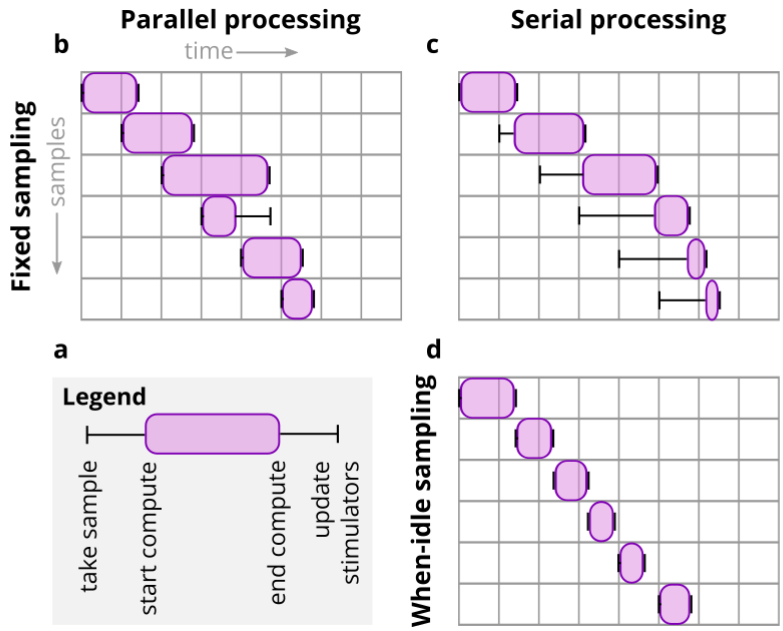

Figure 3.2: Latency emulation strategy and available configurations. (A) Cleo registers the time a sample is taken from the recording devices, the times the computation starts and ends, applying the user-specified delay, and updates stimulation devices when finished. (B) The default, parallel processing/fixed sampling mode. (C) The serial processing/fixed sampling case reflects when computations are not performed in parallel, but sampling continues on a fixed schedule. (D) The final processing mode avoids buffer overflow by sampling only once the computation for the previous step has terminated.

3.2.3 Electrode recording

3.2.3.1 Spiking

Because we have prioritized point neuron simulations, the electrode functionality currently implemented in Cleo does not rely on raw extracellular potentials, which can only be computed from multi-compartment neurons (Buzsáki et al., 2012; Pettersen et al., 2012). This biophysical forward modeling approach has been taken in other software (Hagen et al., 2018; Parasuram et al., 2016; Thornton et al., 2019; Tomsett et al., 2015).

To approximate spike recording without filtering and thresholding of extracellular potentials, Cleo simply takes ground-truth spikes and stochastically determines which to report using a detection probability function. This function is parametrized by a perfect detection radius, within which all spikes are reported, a half detection radius, at which distance there is a 50% chance a spike will be detected, and a cutoff probability, below which all neurons are ignored. The detection probability function is interpolated between the parametrized points with a $1/r$ function (Holt and Koch, 1999; Nason et al., 2020), where r is the distance between the neuron and the electrode (see Figure 3.3).

Cleo provides spike recording functionality in two forms: multi-unit and sorted. Multi-unit spiking reports every spike detected by every channel, without regard for the origin of the spike. Thus, each channel can report spikes from multiple neurons and a single spike can be reported on multiple channels. Sorted spiking reports all spikes detected on at least one channel, where each neuron is identified by a unique index. While real-time spike sorting is currently not feasible in practice for large numbers of contacts, this sorted spiking option could be used to emulate a common workflow of isolating one or a few neurons to report spikes from in real time.

3.2.3.2 LFP

In order to approximate cortical LFP without recurring to morphological neurons and biophysical forward modeling, we implemented the kernel LFP approximation from (Telenczuk et al., 2020), which we term TKLFP (Teleńczuk kernel LFP). This method approximates the per-spike contribution to LFP (termed uLFP: unitary LFP) with a delayed Gaussian function, where amplitude and delay depend on the position of the neuron relative to the electrode. While the original study included reference peak amplitude A_0 values at just four cortical depths, we inferred these values for arbitrary depths by performing cubic interpolation on data from their figure 5 and assumed that this profile dropped to zero at 600 µm below the soma and 1000 µm above. This implementation is available as a standalone Python package on PyPI (Johnsen, 2022). Accuracy of this implementation is verified in automated test suites in both TKLFP and Cleo packages.

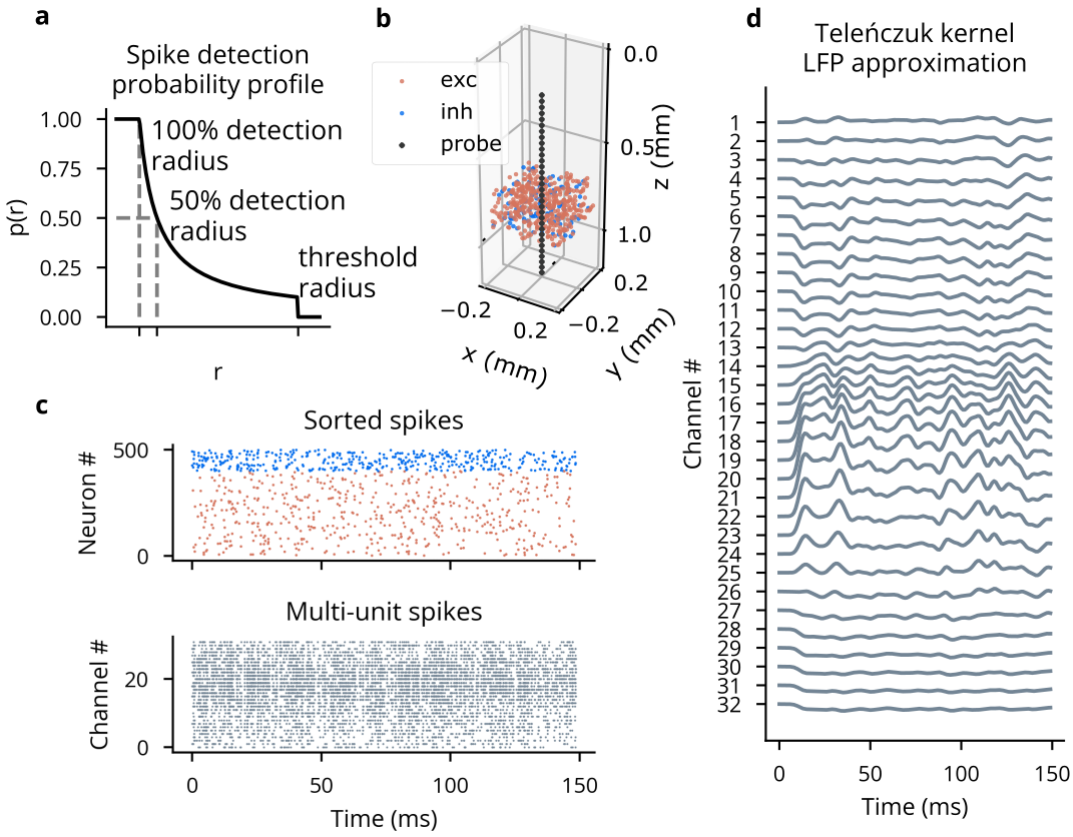

Figure 3.3: Illustration of LFP and spiking from Cleo's electrophysiology module. (A) The probabilistic spike detection model. All spikes within the 100% detection radius, 50% of spikes at the 50% detection radius, and none of those outside the threshold radius are recorded. The detection probability decays with 1/r. (B) An example plot generated by Cleo showing the positions of neurons and electrode contacts. (C) Randomly generated spikes for the neurons shown in B. Top: the sorted spike signal, which gives the ground truth source neuron for every spike as a perfect proxy for spike sorting. Bottom: multi-unit spikes, where spikes are reported on every channel they are detected on, regardless of the source neuron. (D) The TKLFP signal generated from the spikes in C for each channel. Y-axis units are not shown.

3.2.4 Optogenetic stimulation

3.2.4.1 Light model

Cleo simulates optogenetic stimulation by combining a model of light propagation with an opsin model relating light to current. The light model is taken from (Foutz et al., 2012) and uses Kubelka-Munk light propagation. This is a simplified model operating on the assumption that the medium is optically homogeneous, which, while not true, was shown by Foutz et al. to be a suitable approximation. Cleo includes absorbance, scattering, and refraction parameters for blue, 473-nm light as given in (Foutz et al., 2012).

3.2.4.2 Opsin models

Independent of the light propagation model, Cleo provides two different opsin models. One is a four-state Markov model as presented in (Evans et al., 2016), which captures rise, peak, plateau, and fall dynamics as the opsin is activated and deactivated through a Markov process. Additionally, by defining conductance rather than current directly, the model is able to reproduce the photocurrent's dependence on the membrane potential (see Figure 3.4). While the four-state model fits experimental data fairly well, the code is structured so that the three- or six-state models in (Evans et al., 2016) could also be easily implemented.

Because the Markov model depends on somewhat realistic membrane potential and resistance values, however, it is not well suited for many pre-existing models that do not. For example, many commonly used leaky integrate-and-fire (LIF) neurons define the membrane potential as ranging from 0 to 1, rather than -70 mV to -50 mV, rendering both the units and values (relative to the opsin's reversal potential) incompatible. One solution would be for users to adapt their neuron models for compatibility with this Markov opsin model, but since this would be burdensome, we developed an alternative model that simply delivers photocurrent proportional to the light intensity at each neuron. Thus, users can retain their original model with no need to add units or modify parameters.

In addition to options for opsin modeling, Cleo allows the user to specify both the probability that cells of a target population express an opsin and the per-cell expression level. This allows for the study of the impact of heterogeneous expression on the outcome of an experiment.

3.3 Results

3.3.1 Model validation

The light model from (Foutz et al., 2012) was successfully replicated, and the light intensity-firing rate relationship was qualitatively similar to that originally reported, though differing in

some respects. This can be attributed to the use of point neurons rather than morphological neurons. See Figure 3.4 for details. Additionally, preliminary experiments show that the simplified, proportional current opsin model is able to produce a firing response qualitatively similar to that of the Markov model.

3.3.2 Example experiments

In order to demonstrate Cleo's utility to the public, we implemented three example experiments to feature in the upcoming publication:

1. Closed-loop inhibition of a traveling wave in a rodent somatosensory cortex model (Moldakarimov et al., 2018).
2. Feedback control of layer 2/3 interneurons, disrupting plasticity in a model of primary visual cortex (Wilmes and Clopath, 2019).
3. Optogenetic evocation of sharp wave-ripples in an anatomically detailed model of hippocampus (Aussel et al., 2022, 2018). See Figure 3.5 for details, and note that feedback control, not looking ahead, so to speak, fails to evoke the reference signal at the desired time. The strategy I propose in Chapter 4 should remedy this.

3.3.3 Open-source code and documentation

Cleo is open-source and can be installed from the Python Package Index under the name `cleosim`. The code can be found on GitHub. Documentation, including an overview, tutorials, and API reference, can be found at https://cleosim.readthedocs.io.

3.4 Limitations

3.4.1 Guiding principles

Because we prioritize point neuron models, Cleo does not currently provide tools for recording realistic extracellular potentials. This would preclude realistically simulating such methods as spike sorting. Currently, the sorted spikes signal Cleo can record assumes perfect sorting but could be made more realistic by adding sorting noise.

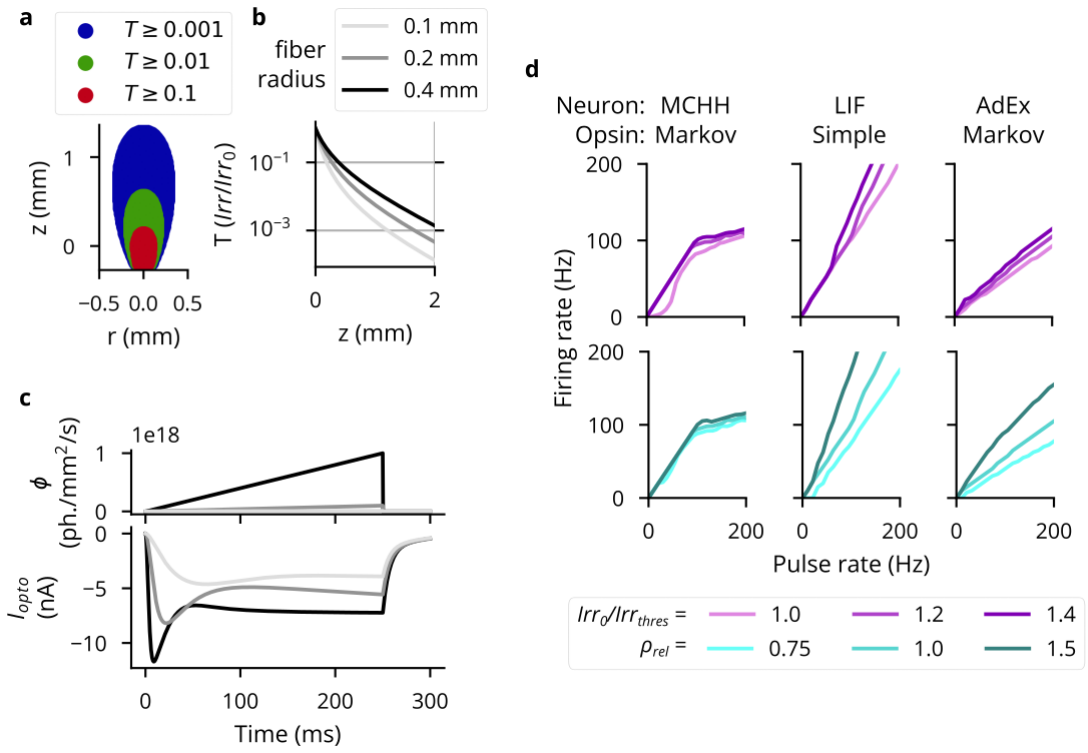

Figure 3.4: Validation of the optogenetics module. (A) Light transmittance T as a function of radius and axial distance from the optic fiber tip. Transmittance refers to the irradiance Irr as a proportion of the irradiance at the fiber tip Irr_0. After Figure 2a from Foutz et al. (2012). (B) Light transmittance T as a function of distance z straight out from the fiber tip for different optic fiber sizes. After Figure 2b from Foutz et al. (2012). (C) Photocurrent I_{opto} for ramping light of different intensities. After the figure produced by the "ramp" protocol from the default PyRhO simulator Evans et al. (2016). (D) Neuron firing rates in response to optical stimulation with 5-ms pulse frequencies ranging from 1 to 200 Hz. The left column re-plots data from Foutz et al. (2012). The middle column shows results for an LIF neuron with a simple opsin, and the right column for a tonic AdEx neuron (Gerstner et al., 2014) with a Markov opsin model. The top row shows results for different light intensities: 100%, 120%, and 140% of the threshold for producing a single spike with a 5-ms pulse. The bottom row shows results for different expression levels relative to the default, ρ_{rel}. The irradiance used for these simulations was 120% of the single-spike threshold.

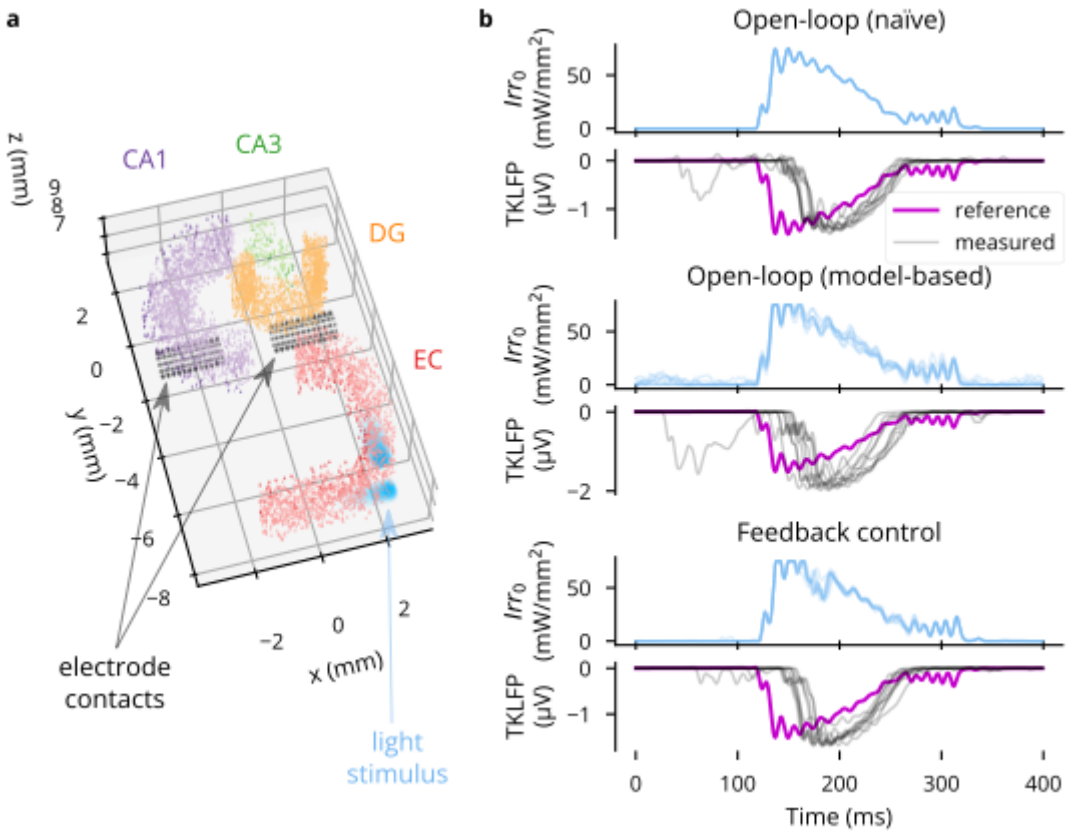

Figure 3.5: An example application of Cleo to the anatomical hippocampus model from Aussel et al. (2022, 2018). (A) A 2.5 mm-thick slice of the 15 mm-tall model is shown. The model consists of four regions, entorhinal cortex (EC), dentate gyrus (DG), CA3, and CA1. Electrode contacts are represented as black dots and are in the same location as in the original model. Two light sources are shown in EC. Nine other such pairs (for a total of 20 light sources) not pictured here were spaced regularly parallel to the z axis. (B) Results are shown for ten trials each of three stimulation paradigms: naïve open-loop, where the input is simply a mirrored, rectified version of the reference signal; model-based open-loop, where a controller is run offline on a simulated model; and feedback control, where a controller is run using online measurements. Input Irr_0 is the light intensity at the tip of each optic fiber. The system output TKLFP refers to the Teleńczuk kernel LFP approximation.

3.4.2 Closed-loop simulation architecture

One downside of using Brian is that it does not have the same first-class support for multi-compartment neurons as the popular NEURON (Hines and Carnevale, 1997) simulator. Using point neurons precludes advanced, morphology-dependent features of neural dynamics as well as recording and stimulation. However, if this feature is needed, Cleo could be developed further to integrate with Brian's morphological neuron features.

Both a strength and a limitation of Cleo's design is that it depends on whatever model the user provides. This avoids the pitfall of painstakingly developing stock models may or may not prove useful to researchers and instead lets them identify or develop a model that adequately describes the phenomena being studied. If a sufficiently realistic model for the studied system does not exist, however, developing one may be prohibitively costly, becoming a computational project in its own right as opposed to simply a stepping-stone towards an experiment. In these cases we suggest that a workaround could be to test a variety of potential models to identify which experimental configurations would be robust to unknown properties of the system. Indeed, the desired experiment in this case could be one that best adjudicates between these hypotheses (**willats-clinc?**).

3.4.3 Electrodes

Using point neurons requires approximation of extraceullar potentials, which do not perfectly match ground-truth signals. The TKLFP approximation Cleo uses, for example, underrepresents high-frequency signals. Fortunately, there is an alternate, potentially more accurate, LFP approximation for point neurons that can be added to Cleo in the future if needed (Mazzoni et al., 2015) and which we are implementing now.

3.4.4 Optogenetics

Currently only channelrhodopsin-2 model parameters are included—comparing the effectiveness of different opsins will require first obtaining parameters. This is important since new opsins have been engineered with improved characteristics (Gunaydin et al., 2010; Hochbaum et al., 2014; Kishi et al., 2022; Klapoetke et al., 2014; Lin et al., 2013; Mager et al., 2018; Sridharan et al., 2022), as well as chloride pumps (Berndt et al., 2016; Chuong et al., 2014; Gradinaru et al., 2010), channels (Govorunova et al., 2017, 2015), and other innovations (Berndt et al., 2016; Vierock et al., 2021)]. Thankfully, parameters for many opsins are available in published literature (Bansal et al., 2021, 2020a, 2020b; Gupta et al., 2019; Saran et al., 2018).

Another limitation is support for multiple simultaneous opsins or light sources. At present, the user could manually include separate current terms for each opsin in neuron model equations or approximate spectral overlap by adding a fraction of a light source's intensity to that of another, but this potentially slow workflow is antithetical to Cleo's goal of requiring minimum

work to test different scenarios. We plan on adding this functionality shortly, since it will be important for Aims 2 and 3.

4 Aim 2: Multi-input CLOC

4.1 Rationale

4.1.1 Advantages of multi-input control

The power of closed-loop optogenetic control (CLOC, henceforth referring specifically to feedback control; see Section 2.1.1) is limited by the degrees of freedom provided by the optogenetic actuation scheme. One important distinction in possible actuation schemes is between unidirectional and bidirectional actuation, referring to whether a single opsin type or both excitatory and inhibitory opsins are used simultaneously. Unidirectional control has obvious shortcomings: for example, an excitatory opsin alone can only raise the firing rate of target neurons, not lower it or even clamp to a baseline level. This setup would also be unable to *lower* the firing rate quickly, in the case of a dynamic reference trajectory. Moreover, besides enabling bidirectional stimulation, general multi-input methods could enable more precise control by targeting different neurons simultaneously, such as stimulation of cells at different depths in a cortical column or across columns.

4.1.2 Advantages of model-based, optimal control

While a previous study (Newman et al., 2015) has already laid the foundation for bidirectional CLOC, it does not feature the generalizability and scalability of the model-based, optimal control algorithms introduced by later work (Bolus et al., 2021) (see Section 2.3) for unidirectional actuation. This adaptive linear-quadratic regulator (LQR) approach is more robust to disturbances and can scale to multi-input multi-output (MIMO) systems. Moreover, its behavior can be easily configured by setting penalties on state error, the control signal, and even the derivative of the control signal to encourage smooth actuation.

4.1.3 Challenges of combining

Thus, a natural goal for furthering CLOC is to combine the advantages of multi-input/bidirectional actuation and model-based optimal control—however, this poses additional challenges and opportunities. The adaptive LQR method previously developed is unsuitable for multi-input actuation because it does not model the constraint that the input (light intensity) must be nonnegative. While violations of this constraint are relatively

infrequent and of little consequence when using an excitatory opsin to reach elevated, slowly varying trajectories, a dual-input scenario would be different. For instance, the controller might call for negative inhibitory input rather than positive excitatory input—a problem that might be solvable with heuristics for the simplest cases but which would pose serious limitations with increasing actuator count.

4.1.4 Innovation

I propose addressing this problem using model predictive control (MPC), which is widely used for its flexibility in implementing optimal control with constraints. Rather than computing the control signal from the current error signal at each step, MPC looks ahead, optimizing over the predicted trajectory some finite number of steps into the future, in what is known as "receding horizon control." I hypothesize that a model predictive strategy will be able to optimize multi-input optogenetic actuation while accommodating experimental constraints and considerations and maintaining low error levels during fast, real-time control. I plan to achieve this aim by adapting previously demonstrated linear models and adding input constraints, demonstrating the advantage of MPC-powered multi-input CLOC *in silico*, and benchmarking algorithm performance to inform future *in-vivo* experiments.

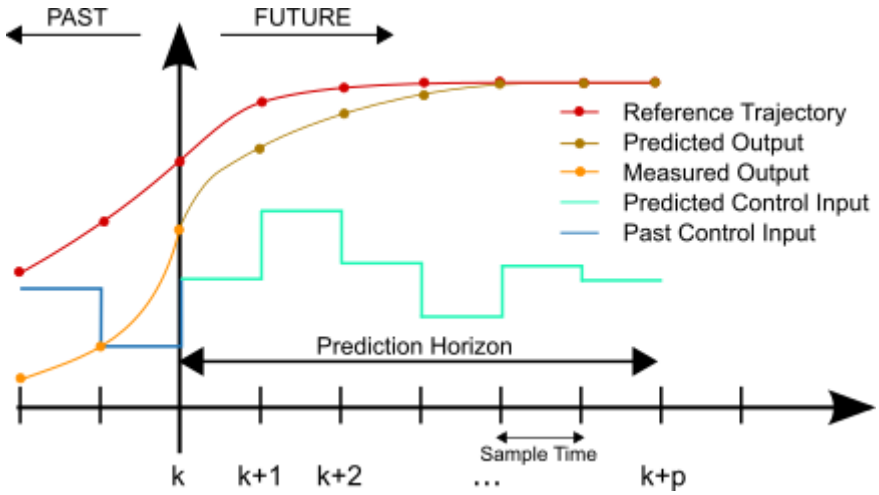

Figure 4.1: An illustration of how MPC optimizes the system input over a receding horizon. By Martin Behrendt, licensed under CC BY-SA 3.0.

4.2 Approach

4.2.1 System and controller formulation

Naturally, the model is a vital element of MPC. I will use a previously developed Gaussian linear dynamical system (GLDS) model (Bolus et al., 2021), which has been shown to reliably capture firing rate dynamics in a light-driven spiking neuron system. The discrete-time GLDS is governed by the following equations:

$$x_{t+1} = Ax_t + Bu_t + w_t \ ,$$

$$y_t = Cx_t + d \ ,$$

$$z_t = y_t + v_t \ ,$$

where $x_t \in \mathbb{R}^n$ is the n-dimensional state, $u_t \in \mathbb{R}^k$ is the k-dimensional stimulus (i.e., $k = 2$ for two opsins, one light source each), $y_t \in \mathbb{R}^m$ is the firing rate in spikes/timestep (for each of m measured neurons), and $z_t \in \mathbb{R}^m$ is the number of binned spikes observed at time t. $A \in \mathbb{R}^{n\times n}$, $B \in \mathbb{R}^{n\times k}$, and $C \in \mathbb{R}^{m\times n}$ are the state transition, input, and output matrices, respectively. $w_t \sim \mathcal{N}(0, Q)$ and $v_t \sim \mathcal{N}(0, R)$ are Gaussian-distributed process and measurement noise, respectively, and $d \in \mathbb{R}^{m\times 1}$ represents baseline firing rates. Model order (n) and horizon length ($T \in \mathbb{N}$) will be chosen to balance complexity and prediction error for noise-driven fitting data generated from the test network. The latent state x_t will be estimated online using the Kalman filter (Kalman, 1960), driven by the prediction error $z_t - \hat{y}_{t|t-1}$.

I will set hard non-negative constraints on the light input as well as a ceiling determined by hardware limitations (i.e., the maximum voltage deliverable to the LED driver). To design an appropriate cost function, I will use a conventional per-time step quadratic form

$$\ell(x_t, r_t, u_t) = (x_t - r_t)^T Q^{\text{ctrl}}(x_t - r_t) + u^T R^{\text{ctrl}} u \ ,$$

where $r_t \in \mathbb{R}^n$ is the reference trajectory at time t. Q^{ctrl} and R^{ctrl} are real $n \times n$ and $k \times k$ matrices chosen to appropriately penalize tracking error and stimulus size, respectively. This quadratic cost function formulation lends the problem well to standard optimization techniques—combined with a linear dynamical system, it constitutes the classical linear-quadratic-Gaussian (LQG) control problem.

Then, at every time step t the controller solves the following quadratic program:

$$\begin{aligned} \text{minimize} \quad & \sum_{\tau=t}^{t+T} \ell(x_\tau, u_\tau) \\ \text{subject to} \quad & u_\tau \succeq 0 \\ & x_{\tau+1} = Ax_\tau + Bu_\tau \end{aligned}$$

where $T \in \mathbb{N}$ is the number of steps in the prediction/control horizon and $\succeq$ indicates an inequality for each element of $u_\tau \in \mathbb{R}^k$. This yields the solution $\tilde{u}_\tau, ..., \tilde{u}_{\tau+T-1}$, of which we take just the first step to apply to the system:

$$u_t = \tilde{u}_t$$

4.2.2 Demonstration of advantages *in silico*

To demonstrate the advantages of control and of MPC, I will control the firing rate of simulated spiking neurons under four conditions: LQR with one opsin, LQR with two opsins, MPC with one opsin and MPC with two opsins. I will test scenarios where the limitations of unidirectional control and LQR will be manifest, namely clamping activity to baseline levels in the presence of unmodeled disturbances to the system and for time-varying reference trajectories. I will also demonstrate the more advanced multi-input applications of MPC by controlling multiple neurons simultaneously with multiple light sources.

All experiments will be performed on a simulated randomly connected network of excitatory and inhibitory leaky integrate-and-fire (LIF) neurons or a Poisson linear dynamical system (Macke et al., 2011) model fit to simulated data. The framework of Aim 1 will be leveraged to simulate electrode recording and optogenetic stimulation, and spikes from individual neurons will be used as inputs to the controller. In all experiments I will compare my MPC approach to the unconstrained LQR controller developed previously (Bolus et al., 2021). I will also compare to an optimal open-loop stimulus computed over a whole-trial horizon. To evaluate controller performance, I will use metrics such as the mean-squared error (MSE) between the reference firing rate and the Gaussian window-smoothed firing rate of the spikes received by the controller during the trial. Noise will be provided to the network where needed to simulate an external disturbance.

4.2.3 Preparation for real-time experiments

To inform future experiments where compute time is crucial for control performance, I will record compute time of LQR and MPC approaches for varying numbers of input and output channels k and m. For instance, the time required to solve the quadratic program for MPC would provide a preliminary estimate of the minimum control period we may want to use when implementing MPC in real time. To get a better idea of how this compute latency might affect

a real experiment, I will also test multi-input MPC on a more realistic simulation, such as one of the example experiments from Section 3.3.2, leveraging the latency simulation capabilities of the CLOC simulation framework.

4.3 Expected results

I expect that bidirectional control will be perform better than unidirectional control at the aforementioned tasks of clamping baseline activities and following a dynamic reference trajectory. I also expect that MPC will attain higher performance than LQR for all multi-input conditions and especially in the case of a dynamic reference. While MPC will be considerably slower than LQR, it should be fast enough for control of neural phenomena on the timescale of hundreds of milliseconds.

4.4 Preliminary results

Basic simulations controlling a linear dynamical system model fit to experimental data show the advantages of bidirectional control and of MPC (see Figure 4.2). Bidirectional actuation allows the system to avoid overshooting the reference, in the case of LQR, or to minimize error faster by first exciting then inhibiting, in the case of MPC. MPC's advantages in looking ahead also clearly allow it to follow the reference more closely than the heuristic LQR controller (assigning negative inputs to the second light source).

4.5 Potential pitfalls & alternative strategies

There are some limitations in the proposed GLDS model that may need to be addressed. While it was adequate for the experiments in Bolus et al. (2021), a Poisson linear dynamical system model (Macke et al., 2011) may be needed in the case that negative predicted firing rates (because the output is not constrained to be nonnegative) produce significant model mismatch error. Also, in case the data is not fit well by a GLDS, I may explore the impact of making parts of the model nonlinear. The output equation $y = Cx + d$, for example, could be replaced by a nonlinear equation of the form $y = f(x)$. While this would likely make the estimation of x more expensive, the underlying dynamics could remain linear, leaving the same underlying quadratic program for the controller to solve.

This touches another potential concern: the speed of the algorithm. If the optimization problem takes too long to solve, there are a few options to explore. One is that some variations in the control scheme can help balance speed and performance, such as letting the control horizon be shorter than the prediction horizon, which shrinks the optimization problem. Likewise, the control period can be longer than the time step of the system, reducing how often the

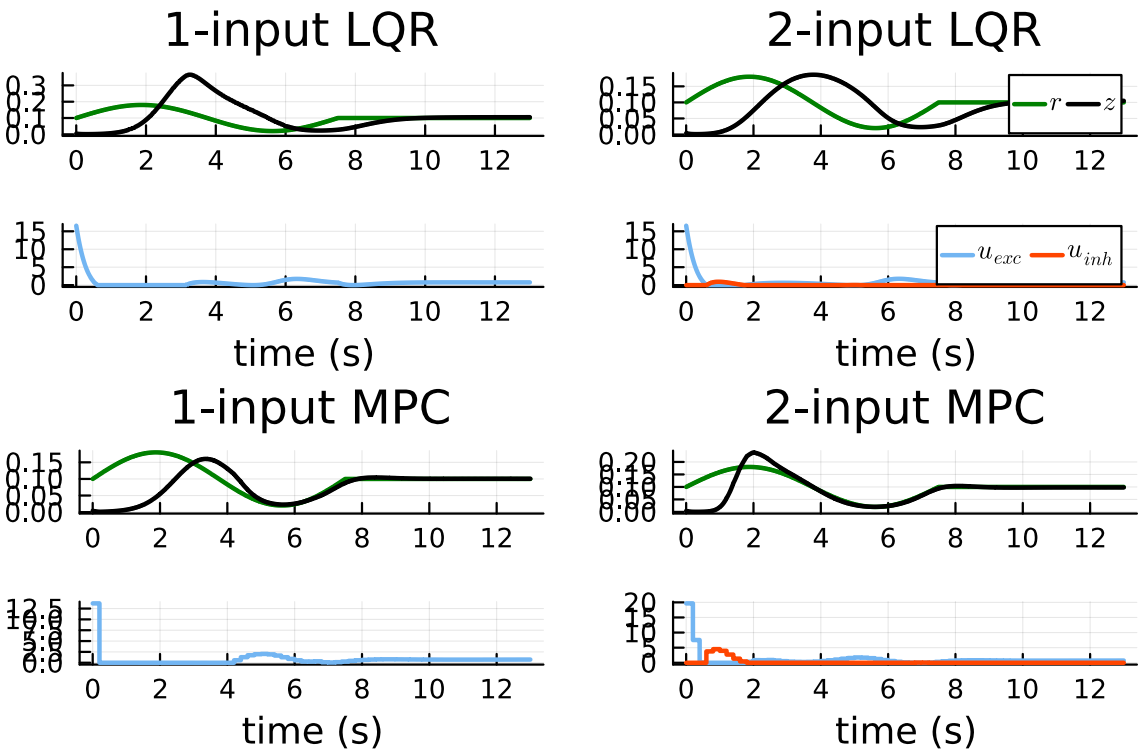

Figure 4.2: Simulated control of an linear dynamical system with 1- and 2-input control, using LQR and MPC controllers. The top panel of each contains the reference and the actual firing rate, in spikes/second. The bottom contains the light intensity, in terms of mW/mm^2, where blue represents light for an excitatory opsin (such as ChR2) and red-orange that for an inhibitory opsin (such as Jaws).

control signal is computed. If conventional methods such as these are unsuccessful, I may turn to methods such as that described in Wang and Boyd (2010) or training an artificial neural network to approximate the exact solution of the quadratic program or to minimize the cost directly. Another potential solution is explicit MPC (Bemporad et al., 2002), which finds a piecewise-affine explicit solution to the quadratic program which can be faster than using a solver to obtain the implicit solution for small-enough problems.

5 Aim 3: Control of latent population dynamics

5.1 Rationale

5.1.1 Success of low-D dynamical models

As technology for recording from the brain has improved, systems neuroscience has shifted increasingly towards a reduced-dimensionality, population coding perspective in many brain areas (Barack and Krakauer, 2021; Churchland et al., 2012; Cunningham and Yu, 2014; Kalaska et al., 1983). This reflects the observation that while the activity of any single neuron can vary greatly across trials where external variables are controlled, underlying latent variables can be decoded from the population which are much more predictable and reproducible. Moreover, formulating this latent variable as a dynamical state whose evolution can be predicted has been shown to improve inference and enable state-of-the-art "decoding" of downstream variables of interest such as movement (Pandarinath et al., 2018; Sani et al., 2021a, 2021b; Willett et al., 2021), mood (Sani et al., 2018), speech (Anumanchipalli et al., 2019), and decision states (Kim et al., 2021; Morcos and Harvey, 2016). Not only does this allow us to infer the output of a given brain region, but it allows us to form hypotheses about how it produces that output by analyzing the dynamical landscape of fixed points (Smith et al., 2021; Sussillo, 2014; Sussillo and Barak, 2013). This is formalized in the Computation through Dynamics (CTD) framework (Vyas et al., 2020).

5.1.2 The need to causally test latent factors

However, while these latent variables have been used to successfully decode other variables of interest, this is a necessary, but insufficent, condition to demonstrate a causal relationship. That is, an association between neural activity variable a and some other variable b may reflect the causal relationship $a \rightarrow b$, but could also reflect $b \rightarrow a$ or $a \leftarrow c \rightarrow b$. This may be adequate for brain-computer interface (BCI) applications, but verification of that causal relationship is necessary for neuroscience's goal of deepening our understanding of the architecture and algorithms of brain computations. This requires experimental control (Pearl, 2009) on the level of neural populations, but, as stated by Vyas et al. (2020),

> The challenge is nontrivial; testing CTD models requires a high degree of control over neural activity. The experimenter must be able to manipulate neural states arbitrarily in state space and then measure behavioral and neural consequences of such perturbations[.]

5.1.3 An ideal application for CLOC

CLOC is a natural candidate for this kind of experimental control of latent states for various reasons. The optimal state-space methods already formulated map directly to the latent dynamics models which have generated so much interest in recent systems neuroscience. High-dimensional optogenetic actuation is possible through micro-LED devices (Antolik et al., 2021; Dufour and Koninck, 2015; Eriksson et al., 2022; Jeon et al., 2021; Kathe et al., 2022; Kwon et al., 2015; Mao et al., 2021; Mao et al., 2019; McAlinden et al., 2019; Ohta et al., 2021; Wang et al., 2018; Welkenhuysen et al., 2016), two-photon targeting of individual neurons (I.-W. Chen et al., 2018; Packer et al., 2015; Ronzitti et al., 2017; Sridharan et al., 2022; Zhang et al., 2018), and genetic targeting. Moreover, real-time feedback can drive a variable neural system towards complex latent state targets which would be attainable with low accuracy at best and not at all at worst with open-loop stimulation [1]. However, while it is clear a high degree of control will be needed, it is unknown how this translates to recording, stimulation, and control parameters. Furthermore, finding optimal parameters would likely require extensive trial and error, as well actuation hardware that does not exist or is not readily available, making it costly if not infeasible to do *in vivo*.

5.1.4 Innovation

Thus, to provide experimenters a proof of concept as well as a point of reference for future *in-vivo* experiments, I propose to develop technical and conceptual guidelines as I control the latent dynamics of simulated neural populations. First, I will produce virtual models by training recurrent spiking neural networks with state-of-the-art, biologically plausible methods—each differing in their degrees of brain-like architecture and training procedure complexity. I will then use the simulation testbed of Aim 1 and the multi-input control methods of Aim 2 to explore how control quality varies with both experimental parameters (such as recording and stimulation channel counts or control algorithms) and system characteristics (such as the size, complexity of the network model)—thus giving researchers a tentative idea of the relative importance of each factor of CLOC.

1: Design task(s)

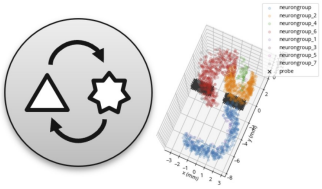

2: Construct spatial RSNN model

3: Train RSNN to perform task

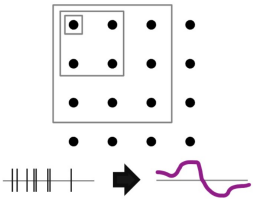

4: Record using Cleo, fit model and decode latent factors, assess decoding quality

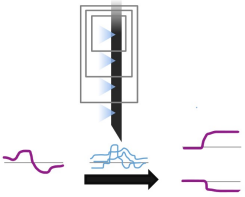

5: Stimulate using Cleo, tune controller and control latent factors, assess control quality

Figure 5.1: Overview of latent factor control experiments.

5.2 Approach

5.2.1 Formulate task with latent dynamics hypothesis

To model an experiment of interest to neuroscientists, I will first choose a task where latent dynamic analyses have yielded testable hypotheses in animal research. For example, it is hypothesized that motor cortex works as a dynamical system where movement planning essentially sets an initial condition during a preparatory phase. This is demonstrated specifically by decoding reach direction in a delayed reach task from dorsal premotor cortex before movement onset (Churchland et al., 2010; reviewed in Gallego et al., 2017) (see Figure 5.2). One way to causally test this hypothesis would be to manipulate the latent factors corresponding to a certain reach direction despite an absent or contradictory cue and verify whether the subject reaches in the predicted direction.

Another potential latent dynamics hypothesis to test could involve sensory integration in decision making. In one "T-maze" task, for example, mice run down a maze, receive a variable number of left and right sensory cues, and at the end choose to go left or right, receiving a reward if they choose the side which they had received more cues from. Morcos and Harvey (2016) find a variety of activity and behavioral patterns for identical evidence presentations

[1]Low accuracy because open-loop stimulation would not counteract spontaneous variability. Inevitable model mismatch would result in open-loop stimulation potentially entirely missing the mark.

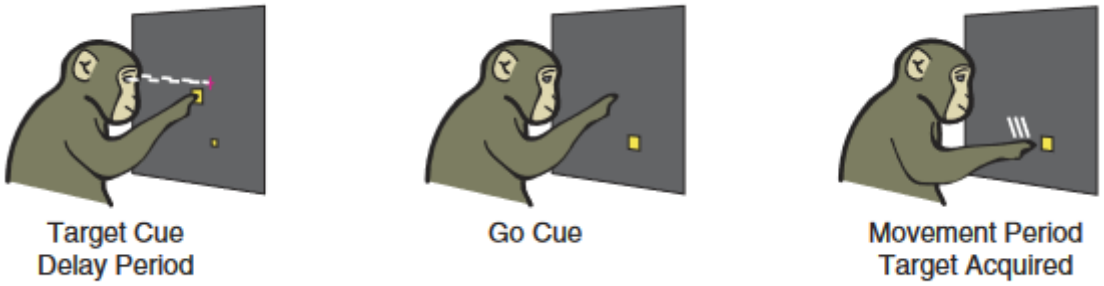

Figure 5.2: Illustration of a delayed center-out reach experiment. From Santhanam et al. (2009).

and attribute it to different initial conditions in the latent space of population activity. Thus, one could test this hypothesis by driving the system to an identical latent state across trials and verifying that this variability goes away. Simply manipulating the latent decision variable to verify that it determines the animal's left or right choice—as opposed to reflecting input from the population(s) actually driving behavior—could be of value as well.

5.2.2 Train RSNN models

After identifying a task and latent dynamics hypothesis to test, I will train recurrent spiking neural network (RSNN) models to perform the task. These RSNN models will be defined in 3D space to make them compatible with the electrode and optogenetics models from Aim 1. To avoid painstaking implementation of every known anatomical detail of the brain region(s) involved in the task—an approach which is not guaranteed to include every important detail or capture true circuitry—I propose using a simple, abstract form such as a rectangular prism of cortical tissue and measuring the effect of adding progressivley more brain-like structural constraints (see Section 5.2.6).

I will then train these models to perform the given task. While a few different methods for training RSNNs exist, I plan on using e-prop (Bellec et al., 2020), a biologically plausible approximation to backpropagation through time (BPTT), the method typically used to train artificial recurrent neural networks (RNNs). This biological plausibility consists in updating synaptic weights using only local information about past activity—"eligibility traces"—and a top-down learning signal and enables learning sparsely firing spike-coding—as opposed to only rate-coding—solutions. While e-prop has been shown to learn complex tasks such as Atari games via reinforcement learning, I propose a simpler supervised learning approach. This is both more data-efficient and would directly allow for the learning of auxiliary variables, which has been shown in one study to make model dynamics more brain-like (Rajalingham et al., 2022) (see Section 5.4).

To give a concrete example of inputs and outputs for the case of the delayed center-out reaching task before mentioned, inputs might include the task phase (stop or go), the target position, and the current hand position. The model output might be hand velocity, and the learning signal could be computed from the x/y distance between the current position and the center (target) before (after) the go cue is given. A regularizer term on acceleration could be added to ensure trajectories are smooth.

5.2.3 Fit dynamical systems model

After a model has been trained to some threshold performance level, I will record spikes and/or LFP from the network while it performs the task. The resulting data will then be used to fit a low-dimensional dynamical systems model. Seeing that the goal of the virtual experiment is to test the causal effect of a latent factor on model output, I propose using system identification methods that prioritize the discovery of those latent factors that are most relevant to behavior. The preferential subspace identification (PSID) method presented by Sani et al. (2021a) is a good candidate, having been shown to predict behavior well with few dimensions. The linear system it produces is also ideal for the control theory methods I develop in Aim 2. In a follow-up study, Sani et al. (2021b) introduce RNN-PSID supporting nonlinearities as well and find empirically that linear dynamics with only a nonlinear mapping from latent to behavior are often sufficient to describe experimental data well. Using a potentially nonlinear output mapping in this way would increase the expressiveness of my models while maintaining underlying linear dynamics for fast optimization.

After fitting a model to data, I will identify latent factors corresponding to variables of interest. These could be individual components of the latent state x directly or simple (e.g., linear) transformations of x. In the delayed center-out reaching task, for example, I would expect two factors with which the state at the end of the preparatory period can be used to predict the cued target position.

5.2.4 Control of latent factors

The next step is then to test whether these latent factors do in fact cause the behavior we observe. Importantly, the model and hypothesis from the previous step were formed without stimulation, since our stated goal is to causally test the latent factors we deduce *from passive observation*. Thus, I will first need to do expand the model by simulating random optogenetic stimulation and fitting an input model—e.g., an input matrix B for the typical LDS case. If this is insufficient to fit the data well, I may need to increase the dimensionality of the latent state x to account for the actuator state (i.e., opsin kinetics) or dimensions of neural activity not arising during unperturbed activity.

With an input model, I will then be able to run control experiments. The methods from Aim 2 will calculate optimal actuation strategies as the simulation progresses to drive the identified

latent factors to the desired state. Control quality will be assessed for each experiment using metrics such as mean-squared error (MSE) and will serve as the criterion for how successful the experiment was, seeing that low error serves the larger goal of testing the causal relationship with model behavior.

5.2.5 Exploration of experiment parameters and expected effects

To guide experimental design, I propose repeating the above process many times to explore how different factors affect control quality, thus informing which investments might be most fruitful. These factors might include:

- *Control type.* Open-loop control is faster and easier but cannot counteract variability inherent to the system and in the presence of model mismatch will fail to reach the target. Closed-loop methods will almost certainly perform better, but are harder to implement. Moreover, closed-loop control offers a range of options spanning the cost/quality spectrum, with the fast linear quadratic regulator (LQR) on one end and the expensive long-horizon, high-resolution model predictive control (MPC) on the other.
- *Total recording/stimulation channel count ($m + k$).* It may be helpful to think of these two parameters together, since they both require limited space in a device that is placed in or on the brain. I expect control quality to increase with channel count up to a point where the computational cost required for closed-loop control outweighs the benefits.
- *Recording/stimulation channel ratio (m/k).* Related to the previous point, when space for interface is hardware, it is an open question whether the current landscape of neuroscience technology, which has prioritized high-channel-count recording over stimulation, is the most effective for causal perturbations of neural dynamics.
- *Data collection budget.* Data collection is not free, and thus must be considered especially when considering the data-efficiency advantages of feedback control. This is also relevant for choosing models to control the system—with little training data, for example, a simple, easy-to-fit model may outperform a more expressive, data-hungry one.
- *Optogenetic stimulation parameters.* These could include the number and type of opsins and genetic targeting. Using at least two opsins could be expected to perform better than just one, as shown in Aim 2, though many more might not be useful due to overlapping spectral sensitivity and increased computation time. The effect of genetic targeting will likely depend on how well the targeted population correlates with the latent factor of interest.

5.2.6 Exploration of model realism and expected effects

As explained above, I propose using abstract RSNN models with varying degrees of brain-like realism rather than extremely detailed models. This is because highly detailed models are difficult to develop and expensive to simulate—moreover, it is hard to say exactly when a

model has enough to detail to behave similarly to a real brain. On the other hand, by assessing the effect of a handful of brain-like features on how well we can contol latent neural dynamics *in silico*, I hope to identify trends that give a rough outlook of doing so *in vivo*. For example, if control quality tends to drop with the addition of each feature, we might infer control of a real brain will be considerably more challenging than in simulations. On the other hand, if control quality does not decrease considerably with brain similarity, we might have reason to be more optimistic.

The brain-like features I propose assessing include structural characteristics such as:

- *Variability.* Brains are far from deterministic, with unpredictability on the level of synaptic transmission all the way up to firing rates across a population. Small-scale stochasticity encourages redundance and robustness, which may make the model harder to "hack," or perturb unnaturally. I expect that large-scale variability, such as an unmodeled input to the region, will highlight the advantages of feedback control.
- *Network size (how many neurons are in the model).* More neurons would likely mean more dimensions along which activity can vary, complicating the prospect of arbitrary control.
- *Subpopulation structure.* This could include constraining connectivity to circuits of brain regions, cortical layers, and cell types. This could also make control harder if the latent factor to control operates in cells that are multiple synapses away from those stimulated or if dynamics become driven by recurrent connections more than stimulation.
- *Connectivity profiles.* Cell pairs within a given population might have a uniform or a spatially dependent connection probability. I expect this, like subpopulation structure, to encourage segregated dynamics which could be either easier or harder to perturb.
- *Cell diversity.* Cells might have uniform or a random distribution of parameters such as membrane resistance, synaptic transmission delays, resting potentials, adaptivity, etc. Again, I expect this would encourage the segregation of neural dynamics.
- *Neuron model complexity.* Individual cell models could range from simple leaky integrate-and-fire (LIF) to Hodgkin-Huxley dynamics. I do not expect this to considerably impact control quality.

They also include characteristics about how the model is trained. A real brain regions is capable of performing not only one, simple, stereotyped task, but many tasks in many contexts. Therefore, another way to make models more brain-like is to diversify their experience—to train them on other tasks. It has been shown that this can result in an RNN reusing computational motifs learned in one task to solve others (Driscoll et al., 2022; Yang et al., 2019).

5.3 Expected results

In addition to the specific expectations for experimental and model parameters described above, I expect that control quality will be relatively low (error will be high) especially for low

actuator counts k. However, I do not anticipate that k will need to approach the per-neuron limit either; rather, that low-error control will be possible with k close to the same order of magnitude as the latent state dimensionality. While expectations for each brain-like model feature are explained above, I predict that on the whole, control quality will decrease as models become more realistic. However, I predict that that that decrease will plateau, providing some level of assurance that the complexity of the real brain may not be an insurmountable barrier to future *in-vivo* experiments.

5.4 Potential pitfalls & alternative strategies

One potential problem is that the RSNN models could learn dynamics that are not very brain-like. For example, they might learn a complicated feedforward function instead of tracking latent variables in a more natural way, in which case explicitly teaching the models to track variables of interest has been shown to make dynamics more brain-like (Rajalingham et al., 2022). Alternatively, the latent variables decoded could be dominated by very few neurons, thus producing "latent variables" which are not actually latent and distributed, as in the brain. This can be avoided by regularizing the state inference step to discourage sparsity, thus inferring the state from a more diverse set of neurons.

Another caveat to generalizing conclusions is that the proposed perturbations may be unnatural—by perturbing the latent factors decoded from passive observation, I may unwittingly by pushing neurons "off-manifold," causing them to fire in unnatural combinations (Shenoy and Kao, 2021). While it is beyond the scope of the proposed work to avoid this, I can at least quantify the phenomenon via the proxy of neural activity *unexplained* by our latent dynamical, assuming our intrinsic manifold is a subspace rather than a lower-dimensional attractor structure embedded therein (Duncker and Sahani, 2021; Vyas et al., 2020). For example, if under passive observation we can predict 95% of neural activity, and that drops to 50% under perturbation, we could conclude that 45% of the activity is now unnatural, as it must be explained by dimensions of activity introduced by stimulation.

Besides conceptual obstacles, the proposed work has practical challenges too—its large scale, to begin with. To adequately assess control prospects across the whole space of experiment and structural factors described could represent a prohibitively high computational cost. This can be mitigated by avoiding a grid search of this space, analyzing random combinations of features or just one at a time rather than every single combination. Another factor in the computational cost is the speed of the training, model fitting, and control simulations themselves. In the case that simulations are too slow with the Brian/Cleo framework described in Aim 1, it may be worth exploring simpler simulations for the training step which does not require Cleo. This could involve using fast differential equation solvers (Rackauckas and Nie, 2017) for the training step or even a less biological learning algorithm such as backpropagation through time with surrogate gradients for the nondifferentiable spike threshold function (Zenke and Vogels, 2021). Training might also be accelerated using a form of "warm start" where weights are initialized

from a pre-trained model, though care would need to be taken that the effects of the warm start on learned dynamics not overshadow those of the structural features being tested.

Additionally, there is a possibility that RNN-PSID requires nonlinear terms to fit model data well, despite the authors' findings that linear dynamics are often sufficient (Sani et al., 2021b). In the case that nonlinearities preclude the formulation of MPC as a fast quadratic program, I may need to turn to neural networks, which, after training, could quickly produce approximate solutions for nonlinear optimization problems (see Section 4.5).

6 Proposed timeline

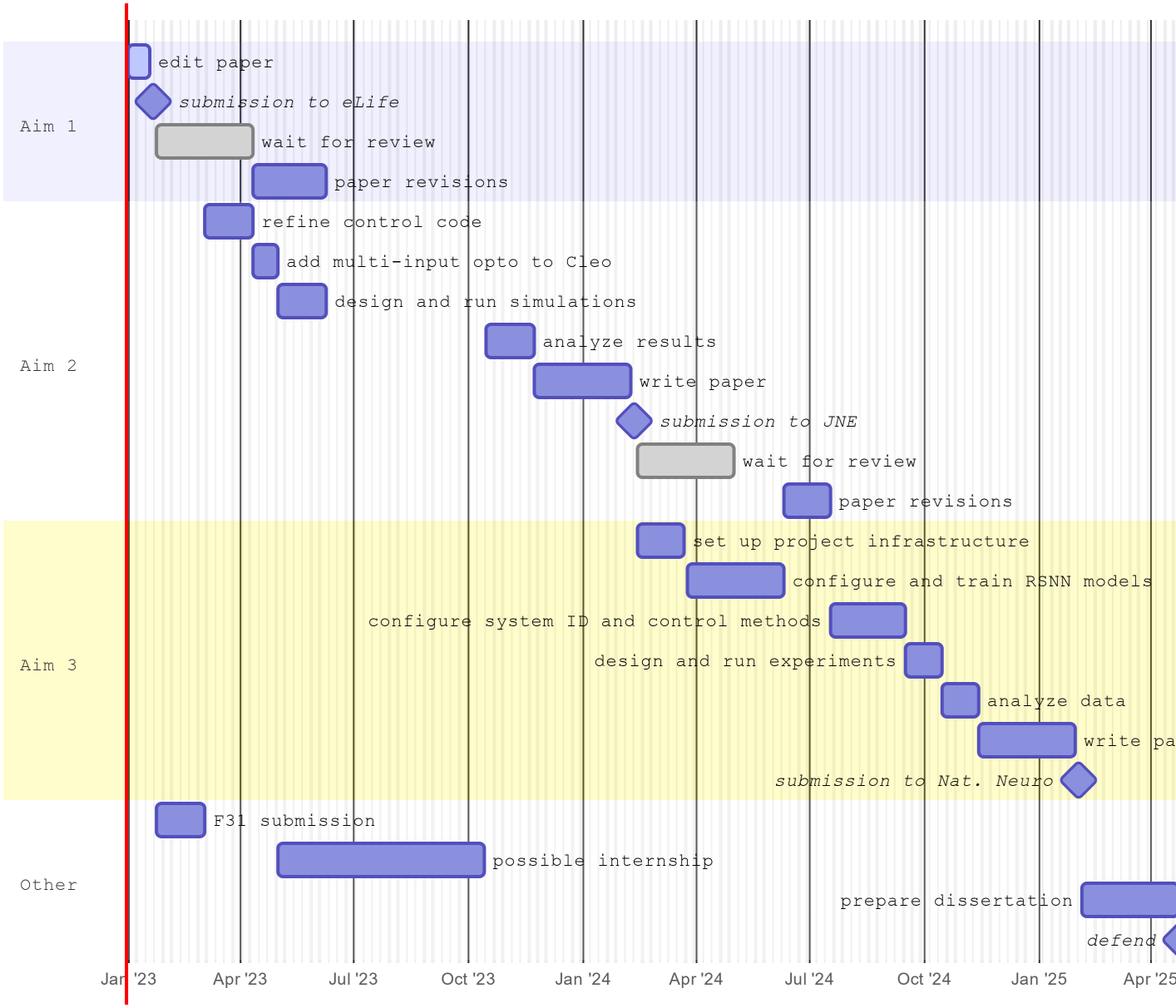

References

Adesnik H, Abdeladim L. 2021. Probing neural codes with two-photon holographic optogenetics. *Nat Neurosci* **24**:1356–1366. doi:10.1038/s41593-021-00902-9

Akam T, Kullmann DM. 2014. Oscillatory multiplexing of population codes for selective communication in the mammalian brain. *Nat Rev Neurosci* **15**:111–122. doi:10.1038/nrn3668

Alegria A, Joshi A, O'Brien J, Kodandaramaiah SB. 2020. Single neuron recording: progress towards high-throughput analysis. *Bioelectron Med (Lond)* **3**:33–36. doi:10.2217/bem-2020-0011

Antolik J, Sabatier Q, Galle C, Frégnac Y, Benosman R. 2021. Assessment of optogenetically-driven strategies for prosthetic restoration of cortical vision in large-scale neural simulation of V1. *Scientific Reports* **11**:1–18. doi:10.1038/s41598-021-88960-8

Anumanchipalli GK, Chartier J, Chang EF. 2019. Speech synthesis from neural decoding of spoken sentences. *Nature* **568**:493–498. doi:10.1038/s41586-019-1119-1

Aru J, Aru J, Priesemann V, Wibral M, Lana L, Pipa G, Singer W, Vicente R. 2015. Untangling cross-frequency coupling in neuroscience. *Current Opinion in Neurobiology* **31**:51–61. doi:10.1016/j.conb.2014.08.002

Aussel A, Buhry L, Tyvaert L, Ranta R. 2018. A detailed anatomical and mathematical model of the hippocampal formation for the generation of sharp-wave ripples and theta-nested gamma oscillations. *J Comput Neurosci* **45**:207–221. doi:10.1007/s10827-018-0704-x

Aussel A, Ranta R, Aron O, Colnat-Coulbois S, Maillard L, Buhry L. 2022. Cell to network computational model of the epileptic human hippocampus suggests specific roles of network and channel dysfunctions in the ictal and interictal oscillations. *J Comput Neurosci*. doi:10.1007/s10827-022-00829-5

Avitan L, Stringer C. 2022. Not so spontaneous: Multi-dimensional representations of behaviors and context in sensory areas. *Neuron*. doi:10.1016/j.neuron.2022.06.019

Bansal H, Gupta N, Roy S. 2021. Theoretical analysis of optogenetic spiking with ChRmine, bReaChES and CsChrimson-expressing neurons for retinal prostheses. *Journal of Neural Engineering* **18**:0460b8. doi:10.1088/1741-2552/ac1175

Bansal H, Gupta N, Roy S. 2020a. Theoretical Analysis of Low-power Bidirectional Optogenetic Control of High-frequency Neural Codes with Single Spike Resolution. *Neuroscience* **449**:165–188. doi:10.1016/j.neuroscience.2020.09.022

Bansal H, Gupta N, Roy S. 2020b. Comparison of low-power, high-frequency and temporally precise optogenetic inhibition of spiking in NpHR, eNpHR3.0 and Jaws-expressing neurons. *Biomedical Physics and Engineering Express* **6**:045011. doi:10.1088/2057-1976/ab90a1

Barack DL, Krakauer JW. 2021. Two views on the cognitive brain. *Nat Rev Neurosci* **22**:359–371. doi:10.1038/s41583-021-00448-6

Bellec G, Scherr F, Subramoney A, Hajek E, Salaj D, Legenstein R, Maass W. 2020. A solution to the learning dilemma for recurrent networks of spiking neurons. *Nature Communications* **11**. doi:10.1101/738385

Bemporad A, Morari M, Dua V, Pistikopoulos EN. 2002. The explicit linear quadratic regulator for constrained systems. *Automatica* **38**:3–20. doi:10.1016/S0005-1098(01)00174-1

Berman GJ, Choi DM, Bialek W, Shaevitz JW. 2014. Mapping the stereotyped behaviour of freely moving fruit flies. *Journal of The Royal Society Interface* **11**:20140672. doi:10.1098/rsif.2014.0672

Berndt A, Lee SY, Wietek J, Ramakrishnan C, Steinberg EE, Rashid AJ, Kim H, Park S, Santoro A, Frankland PW, Iyer SM, Pak S, Ährlund-Richter S, Delp SL, Malenka RC, Josselyn SA, Carlén M, Hegemann P, Deisseroth K. 2016. Structural foundations of optogenetics: Determinants of channelrhodopsin ion selectivity. *Proceedings of the National Academy of Sciences of the United States of America* **113**:822–829. doi:10.1073/pnas.1523341113

Bogdanchikov A, Zhaparov M, Suliyev R. 2013. Python to learn programmingJournal of Physics: Conference Series. IOP Publishing. p. 012027. doi:10.1088/1742-6596/423/1/012027

Bolus MF, Willats AA, Rozell CJ, Stanley GB. 2021. State-space optimal feedback control of optogenetically driven neural activity. *Journal of neural engineering* **18**:036006. doi:10.1101/2020.06.25.171785

Bolus MF, Willats AA, Whitmire CJ, Rozell CJ, Stanley GB. 2018. Design strategies for dynamic closed-loop optogenetic neurocontrol in vivo. *Journal of Neural Engineering* **15**:026011. doi:10.1088/1741-2552/aaa506

Buffalo EA, Fries P, Landman R, Buschman TJ, Desimone R. 2011. Laminar differences in gamma and alpha coherence in the ventral stream. *Proceedings of the National Academy of Sciences of the United States of America* **108**:11262–11267. doi:10.1073/pnas.1011284108

Buschman TJ, Denovellis EL, Diogo C, Bullock D, Miller EK. 2012. Synchronous Oscillatory Neural Ensembles for Rules in the Prefrontal Cortex. *Neuron* **76**:838–846. doi:10.1016/j.neuron.2012.09.029

Buzsáki G. 2015. Hippocampal sharp wave-ripple: A cognitive biomarker for episodic memory and planning. *Hippocampus* **25**:1073–1188. doi:10.1002/hipo.22488

Buzsáki G, Anastassiou CA, Koch C. 2012. The origin of extracellular fields and currents — EEG, ECoG, LFP and spikes. *Nature Reviews Neuroscience 2012 13:6* **13**:407–420. doi:10.1038/nrn3241

Buzsáki G, Draguhn A. 2004. Neuronal oscillations in cortical networks. *Science* **304**:1926–1929. doi:10.1126/science.1099745

Cardin JA, Carlén M, Meletis K, Knoblich U, Zhang F, Deisseroth K, Tsai LH, Moore CI. 2010. Targeted optogenetic stimulation and recording of neurons in vivo using cell-type-specific expression of Channelrhodopsin-2. *Nature Protocols* **5**:247–254. doi:10.1038/nprot.2009.228

Chen I-W, Papagiakoumou E, Emiliani V. 2018. Towards circuit optogenetics. *Current Opinion in Neurobiology*, Neurotechnologies **50**:179–189. doi:10.1016/j.conb.2018.03.008

Chen S, Weitemier AZ, Zeng X, He L, Wang X, Tao Y, Huang AJY, Hashimotodani Y, Kano M, Iwasaki H, Parajuli LK, Okabe S, Loong Teh DB, All AH, Tsutsui-Kimura I, Tanaka

KF, Liu X, McHugh TJ. 2018. Near-infrared deep brain stimulation via upconversion nanoparticle–mediated optogenetics. *Science* **359**:679–684. doi:10.1126/science.aaq1144

Chuong AS, Miri ML, Busskamp V, Matthews GAC, Acker LC, Sørensen AT, Young A, Klapoetke NC, Henninger MA, Kodandaramaiah SB, Ogawa M, Ramanlal SB, Bandler RC, Allen BD, Forest CR, Chow BY, Han X, Lin Y, Tye KM, Roska B, Cardin JA, Boyden ES. 2014. Noninvasive optical inhibition with a red-shifted microbial rhodopsin. *Nature Neuroscience* **17**:1123–1129. doi:10.1038/nn.3752

Churchland MM, Cunningham JP, Kaufman MT, Foster JD, Nuyujukian P, Ryu SI, Shenoy KV, Shenoy KV. 2012. Neural population dynamics during reaching. *Nature* **487**:51–56. doi:10.1038/nature11129

Churchland MM, Cunningham JP, Kaufman MT, Ryu SI, Shenoy KV. 2010. Cortical Preparatory Activity: Representation of Movement or First Cog in a Dynamical Machine? *Neuron* **68**:387–400. doi:10.1016/j.neuron.2010.09.015

Cole SR, Voytek B. 2017. Brain Oscillations and the Importance of Waveform Shape. *Trends in Cognitive Sciences* **21**:137–149. doi:10.1016/j.tics.2016.12.008

Cole S, Voytek B. 2019. Cycle-by-cycle analysis of neural oscillations. *Journal of Neurophysiology* **122**:849–861. doi:10.1152/JN.00273.2019

Cowley BR, Snyder AC, Acar K, Williamson RC, Yu BM, Smith MA. 2020. Slow Drift of Neural Activity as a Signature of Impulsivity in Macaque Visual and Prefrontal Cortex. *Neuron* **108**:551–567.e8. doi:10.1016/j.neuron.2020.07.021

Cunningham JP, Yu BM. 2014. Dimensionality reduction for large-scale neural recordings. *Nature neuroscience* **17**:1500–9. doi:10.1038/nn.3776

Davie JT, Kole MHP, Letzkus JJ, Rancz EA, Spruston N, Stuart GJ, Häusser M. 2006. Dendritic patch-clamp recording. *Nature Protocols* **1**:1235–1247. doi:10.1038/nprot.2006.164

Davis ZW, Muller L, Martinez-Trujillo J, Sejnowski T, Reynolds JH. 2020. Spontaneous travelling cortical waves gate perception in behaving primates. *Nature* **587**:432–436. doi:10.1038/s41586-020-2802-y

Davison AP, Hines ML, Muller E. 2009. Trends in programming languages for neuroscience simulations. *Frontiers in Neuroscience* **3**:374–380. doi:10.3389/neuro.01.036.2009

Driscoll L, Shenoy K, Sussillo D. 2022. Flexible multitask computation in recurrent networks utilizes shared dynamical motifs. doi:10.1101/2022.08.15.503870

Dufour S, Koninck YD. 2015. Optrodes for combined optogenetics and electrophysiology in live animals. *NPh* **2**:031205. doi:10.1117/1.NPh.2.3.031205

Duncker L, Sahani M. 2021. Dynamics on the manifold: Identifying computational dynamical activity from neural population recordings. *Current Opinion in Neurobiology*, Computational Neuroscience **70**:163–170. doi:10.1016/j.conb.2021.10.014

Dutta S, Ackermann E, Kemere C. 2019. Analysis of an open source, closed-loop, realtime system for hippocampal sharp-wave ripple disruption. *Journal of Neural Engineering* **16**:016009. doi:10.1088/1741-2552/aae90e

Emiliani V, Cohen AE, Deisseroth K, Häusser M. 2015. All-optical interrogation of neural circuits. *Journal of Neuroscience* **35**:13917–13926. doi:10.1523/JNEUROSCI.2916-15.2015

Engel D. 2016. Subcellular patch-clamp recordings from the somatodendritic domain of nigral dopamine neurons. *Journal of Visualized Experiments* **2016**:e54601. doi:10.3791/54601

Eriksson D, Schneider A, Thirumalai A, Alyahyay M, de la Crompe B, Sharma K, Ruther P, Diester I. 2022. Multichannel optogenetics combined with laminar recordings for ultra-controlled neuronal interrogation. *Nat Commun* **13**:985. doi:10.1038/s41467-022-28629-6

Evans BD, Jarvis S, Schultz SR, Nikolic K. 2016. PyRhO: A Multiscale Optogenetics Simulation Platform. *Frontiers in Neuroinformatics* **10**:8. doi:10.3389/fninf.2016.00008

Fabus MS, Quinn AJ, Warnaby CE, Woolrich MW. 2021. Automatic decomposition of electrophysiological data into distinct nonsinusoidal oscillatory modes. *Journal of Neurophysiology* **126**:1670–1684. doi:10.1152/jn.00315.2021

Faini G, Molinier C, Telliez C, Tourain C, Forget BC, Ronzitti E, Emiliani V. 2021. Ultrafast Light Targeting for High-Throughput Precise Control of Neuronal Networks. *bioRxiv* 2021.06.14.448315. doi:10.1101/2021.06.14.448315

Fenno L, Yizhar O, Deisseroth K. 2011. The development and application of optogenetics. *Annual Review of Neuroscience* **34**:389–412. doi:10.1146/annurev-neuro-061010-113817

Fernandez LMJ, Lüthi A. 2020. Sleep Spindles: Mechanisms and Functions. *Physiological Reviews* **100**:805–868. doi:10.1152/physrev.00042.2018

Flytzanis NC, Bedbrook CN, Chiu H, Engqvist MKM, Xiao C, Chan KY, Sternberg PW, Arnold FH, Gradinaru V. 2014. Archaerhodopsin variants with enhanced voltage-sensitive fluorescence in mammalian and Caenorhabditis elegans neurons. *Nat Commun* **5**:4894. doi:10.1038/ncomms5894

Foutz TJ, Arlow RL, Mcintyre CC. 2012. Theoretical principles underlying optical stimulation of a channelrhodopsin-2 positive pyramidal neuron. *J Neurophysiol* **107**:3235–3245. doi:10.1152/jn.00501.2011.-Optogenetics

Gallego JA, Perich MG, Miller LE, Solla SA. 2017. Neural Manifolds for the Control of Movement. *Neuron* **94**:978–984. doi:10.1016/j.neuron.2017.05.025

Gerstner W, Kistler WM, Naud R, Paninski L. 2014. Neuronal dynamics: From single neurons to networks and models of cognition. Cambridge University Press. doi:10.1017/CBO9781107447615

Göbel W, Helmchen F. 2007. In Vivo Calcium Imaging of Neural Network Function. *Physiology* **22**:358–365. doi:10.1152/physiol.00032.2007

Govorunova EG, Sineshchekov OA, Janz R, Liu X, Spudich JL. 2015. Natural light-gated anion channels: A family of microbial rhodopsins for advanced optogenetics. *Science* **349**:647–650. doi:10.1126/science.aaa7484

Govorunova EG, Sineshchekov OA, Rodarte EM, Janz R, Morelle O, Melkonian M, Wong GKS, Spudich JL. 2017. The Expanding Family of Natural Anion Channelrhodopsins Reveals Large Variations in Kinetics, Conductance, and Spectral Sensitivity. *Scientific Reports* **7**:1–10. doi:10.1038/srep43358

Gradinaru V, Zhang F, Ramakrishnan C, Mattis J, Prakash R, Diester I, Goshen I, Thompson KR, Deisseroth K. 2010. Molecular and Cellular Approaches for Diversifying and Extending Optogenetics. *Cell* **141**:154–165. doi:10.1016/j.cell.2010.02.037

Grosenick L, Marshel JH, Deisseroth K. 2015. Review Closed-Loop and Activity-Guided Optogenetic Control. *Neuron* **86**:106–139. doi:10.1016/j.neuron.2015.03.034

Gunaydin LA, Yizhar O, Berndt A, Sohal VS, Deisseroth K, Hegemann P. 2010. Ultrafast optogenetic control. *Nature Neuroscience* **13**:387–392. doi:10.1038/nn.2495

Gupta N, Bansal H, Roy S. 2019. Theoretical optimization of high-frequency optogenetic spiking of red-shifted very fast-Chrimson-expressing neurons. *Neurophotonics* **6**:1. doi:10.1117/1.nph.6.2.025002

Gutruf P, Rogers JA. 2018. Implantable, wireless device platforms for neuroscience research. *Current Opinion in Neurobiology*, Neurotechnologies **50**:42–49. doi:10.1016/j.conb.2017.12.007

Hagen E, Næss S, Ness TV, Einevoll GT. 2018. Multimodal modeling of neural network activity: Computing LFP, ECoG, EEG, and MEG signals with LFPy 2.0. *Frontiers in Neuroinformatics* **12**:92. doi:10.3389/fninf.2018.00092

Hines ML, Carnevale NT. 1997. The NEURON Simulation Environment. *Neural Computation* **9**:1179–1209. doi:10.1162/neco.1997.9.6.1179

Hochbaum DR, Zhao Y, Farhi SL, Klapoetke N, Werley CA, Kapoor V, Zou P, Kralj JM, MacLaurin D, Smedemark-Margulies N, Saulnier JL, Boulting GL, Straub C, Cho YK, Melkonian M, Wong GKS, Harrison DJ, Murthy VN, Sabatini BL, Boyden ES, Campbell RE, Cohen AE. 2014. All-optical electrophysiology in mammalian neurons using engineered microbial rhodopsins. *Nature Methods* **11**:825–833. doi:10.1038/NMETH.3000

Hodgkin AL, Huxley AF. 1952. A quantitative description of membrane current and its application to conduction and excitation in nerve. *The Journal of Physiology* **117**:500–544. doi:10.1113/jphysiol.1952.sp004764

Hodgkin AL, Huxley AF, Katz B. 1952. Measurement of current-voltage relations in the membrane of the giant axon of Loligo. *J Physiol* **116**:424–448.

Holt GR, Koch C. 1999. Electrical interactions via the extracellular potential near cell bodies. *Journal of Computational Neuroscience* **6**:169–184. doi:10.1023/A:1008832702585

Hurwitz C, Srivastava A, Xu K, Jude J, Perich MG, Miller LE, Hennig MH. 2021. Targeted Neural Dynamical ModelingAdvances in Neural Information Processing Systems. pp. 29379–29392.

Inoue M. 2021. Genetically encoded calcium indicators to probe complex brain circuit dynamics in vivo. *Neuroscience Research* **169**:2–8. doi:10.1016/j.neures.2020.05.013

Jazayeri M, Ostojic S. 2021. Interpreting neural computations by examining intrinsic and embedding dimensionality of neural activity. *Current Opinion in Neurobiology* **70**:113–120. doi:10.1016/j.conb.2021.08.002

Jeon S, Lee Y, Ryu D, Cho YK, Lee Y, Jun SB, Ji C-H. 2021. Implantable Optrode Array for Optogenetic Modulation and Electrical Neural Recording. *Micromachines* **12**:725. doi:10.3390/mi12060725

Joglekar A, Prjibelski A, Mahfouz A, Collier P, Lin S, Schlusche AK, Marrocco J, Williams SR, Haase B, Hayes A, Chew JG, Weisenfeld NI, Wong MY, Stein AN, Hardwick SA, Hunt T, Wang Q, Dieterich C, Bent Z, Fedrigo O, Sloan SA, Risso D, Jarvis ED, Flicek P, Luo W, Pitt GS, Frankish A, Smit AB, Ross ME, Tilgner HU. 2021. A spatially resolved brain region- and cell type-specific isoform atlas of the postnatal mouse brain. *Nat Commun* **12**:463. doi:10.1038/s41467-020-20343-5

Johnsen K. 2022. kjohnsen/tklfp: v0.2.0. doi:10.5281/zenodo.6787979

Juavinett AL, Bekheet G, Churchland AK. 2019. Chronically implanted Neuropixels probes enable high-yield recordings in freely moving mice. *eLife* **8**:e47188. doi:10.7554/eLife.47188

Kalaska JF, Caminiti R, Georgopoulos AP. 1983. Cortical mechanisms related to the direction

of two-dimensional arm movements: relations in parietal area 5 and comparison with motor cortex. *Exp Brain Res* **51**:247–260. doi:10.1007/BF00237200

Kalman RE. 1960. A new approach to linear filtering and prediction problems. *Journal of Fluids Engineering, Transactions of the ASME* **82**:35–45. doi:10.1115/1.3662552

Karvat G, Schneider A, Alyahyay M, Steenbergen F, Tangermann M, Diester I. 2020. Real-time detection of neural oscillation bursts allows behaviourally relevant neurofeedback. *Commun Biol* **3**:1–10. doi:10.1038/s42003-020-0801-z

Kathe C, Michoud F, Schönle P, Rowald A, Brun N, Ravier J, Furfaro I, Paggi V, Kim K, Soloukey S, Asboth L, Hutson TH, Jelescu I, Philippides A, Alwahab N, Gandar J, Huber D, De Zeeuw CI, Barraud Q, Huang Q, Lacour SP, Courtine G. 2022. Wireless closed-loop optogenetics across the entire dorsoventral spinal cord in mice. *Nat Biotechnol* **40**:198–208. doi:10.1038/s41587-021-01019-x

Kaufman MT, Churchland MM, Ryu SI, Shenoy KV. 2014. Cortical activity in the null space: Permitting preparation without movement. *Nature Neuroscience* **17**:440–448. doi:10.1038/nn.3643

Kazemipour A, Novak O, Flickinger D, Marvin JS, Abdelfattah AS, King J, Borden PM, Kim JJ, Al-Abdullatif SH, Deal PE, Miller EW, Schreiter ER, Druckmann S, Svoboda K, Looger LL, Podgorski K. 2019. Kilohertz frame-rate two-photon tomography. *Nature Methods* **16**:778–786. doi:10.1038/s41592-019-0493-9

Kim TD, Luo TZ, Pillow JW, Brody CD. 2021. Inferring Latent Dynamics Underlying Neural Population Activity via Neural Differential EquationsProceedings of the 38th International Conference on Machine Learning. PMLR. pp. 5551–5561.

Kishi KE, Kim YS, Fukuda M, Inoue M, Kusakizako T, Wang PY, Ramakrishnan C, Byrne EFX, Thadhani E, Paggi JM, Matsui TE, Yamashita K, Nagata T, Konno M, Quirin S, Lo M, Benster T, Uemura T, Liu K, Shibata M, Nomura N, Iwata S, Nureki O, Dror RO, Inoue K, Deisseroth K, Kato HE. 2022. Structural basis for channel conduction in the pump-like channelrhodopsin ChRmine. *Cell* **185**:672–689.e23. doi:10.1016/j.cell.2022.01.007

Klapoetke NC, Murata Y, Kim SS, Pulver SR, Birdsey-Benson A, Cho YK, Morimoto TK, Chuong AS, Carpenter EJ, Tian Z, Wang J, Xie Y, Yan Z, Zhang Y, Chow BY, Surek B, Melkonian M, Jayaraman V, Constantine-Paton M, Wong GKS, Boyden ES. 2014. Independent optical excitation of distinct neural populations. *Nature Methods* **11**:338–346. doi:10.1038/nmeth.2836

Knöpfel T, Song C. 2019. Optical voltage imaging in neurons: moving from technology development to practical tool. *Nat Rev Neurosci* **20**:719–727. doi:10.1038/s41583-019-0231-4

Krook-Magnuson E, Armstrong C, Oijala M, Soltesz I. 2013. On-demand optogenetic control of spontaneous seizures in temporal lobe epilepsy. *Nature Communications* **4**:1–8. doi:10.1038/ncomms2376

Kumar A, Vlachos I, Aertsen A, Boucsein C. 2013. Challenges of understanding brain function by selective modulation of neuronal subpopulations. *Trends in Neurosciences* **36**:579–586. doi:10.1016/j.tins.2013.06.005

Kwon KY, Lee H-M, Ghovanloo M, Weber A, Li W. 2015. Design, fabrication, and packaging of an integrated, wirelessly-powered optrode array for optogenetics application. *Frontiers in Systems Neuroscience* **9**.

Lee C, Lavoie A, Liu J, Chen SX, Liu B. 2020. Light Up the Brain: The Application of Optogenetics in Cell-Type Specific Dissection of Mouse Brain Circuits. *Frontiers in Neural Circuits* **14**.

Lin JY, Knutsen PM, Muller A, Kleinfeld D, Tsien RY. 2013. ReaChR: A red-shifted variant of channelrhodopsin enables deep transcranial optogenetic excitation. *Nature Neuroscience* **16**:1499–1508. doi:10.1038/nn.3502

Lundqvist M, Rose J, Brincat SL, Warden MR, Buschman TJ, Herman P, Miller EK. 2022. Reduced variability of bursting activity during working memory. *Sci Rep* **12**:15050. doi:10.1038/s41598-022-18577-y

Lundqvist M, Rose J, Herman P, Brincat SLL, Buschman TJJ, Miller EKK. 2016. Gamma and Beta Bursts Underlie Working Memory. *Neuron* **90**:152–164. doi:10.1016/j.neuron.2016.02.028

Maaten L van der, Hinton G. 2008. Visualizing Data using t-SNE. *Journal of Machine Learning Research* **9**:2579–2605.

Macke JH, Buesing L, Cunningham JP, Yu BM, Shenoy KV, Sahani M. 2011. Empirical models of spiking in neural populationsAdvances in Neural Information Processing Systems. Curran Associates, Inc.

Mager T, Morena DLDL, Senn V, Schlotte J, Derrico A, Feldbauer K, Wrobel C, Jung S, Bodensiek K, Rankovic V, Browne L, Huet A, Jüttner J, Wood PG, Letzkus JJ, Moser T, Bamberg E. 2018. High frequency neural spiking and auditory signaling by ultrafast red-shifted optogenetics. *Nature Communications* **9**:1–14. doi:10.1038/s41467-018-04146-3

Mao D, Li N, Xiong Z, Sun Y, Xu G. 2019. Single-Cell Optogenetic Control of Calcium Signaling with a High-Density Micro-LED Array. *iScience* **21**:403–412. doi:10.1016/j.isci.2019.10.024

Mao D, Xiong Z, Donnelly M, Xu G. 2021. Brushing-Assisted Two-Color Quantum-Dot Micro-LED Array Towards Bi-Directional Optogenetics. *IEEE Electron Device Letters* **42**:1504–1507. doi:10.1109/LED.2021.3108554

Martinez-Garcia RI, Voelcker B, Zaltsman JB, Patrick SL, Stevens TR, Connors BW, Cruikshank SJ. 2020. Two dynamically distinct circuits drive inhibition in the sensory thalamus. *Nature* **583**:813–818. doi:10.1038/s41586-020-2512-5

Mathis A, Mamidanna P, Cury KM, Abe T, Murthy VN, Mathis MW, Bethge M. 2018. DeepLabCut: markerless pose estimation of user-defined body parts with deep learning. *Nat Neurosci* **21**:1281–1289. doi:10.1038/s41593-018-0209-y

Mazzoni A, Lindén H, Cuntz H, Lansner A, Panzeri S, Einevoll GT. 2015. Computing the Local Field Potential (LFP) from Integrate-and-Fire Network Models. *PLOS Computational Biology* **11**:e1004584. doi:10.1371/JOURNAL.PCBI.1004584

McAlinden N, Cheng Y, Scharf R, Xie E, Gu E, Reiche CF, Sharma R, Tathireddy P, Tathireddy P, Rieth L, Blair S, Mathieson K. 2019. Multisite microLED optrode array for neural interfacing. *NPh* **6**:035010. doi:10.1117/1.NPh.6.3.035010

Moldakarimov S, Bazhenov M, Feldman DE, Sejnowski TJ. 2018. Structured networks support sparse traveling waves in rodent somatosensory cortex. *Proceedings of the National Academy of Sciences of the United States of America* **115**:5277–5282. doi:10.1073/pnas.1710202115

Morcos AS, Harvey CD. 2016. History-dependent variability in population dynamics during

evidence accumulation in cortex. *Nat Neurosci* **19**:1672–1681. doi:10.1038/nn.4403
Mukamel EA, Ngai J. 2019. Perspectives on defining cell types in the brain. *Current Opinion in Neurobiology*, Neuronal Identity **56**:61–68. doi:10.1016/j.conb.2018.11.007
Muller E, Bednar JA, Diesmann M, Gewaltig MO, Hines M, Davison AP. 2015. Python in neuroscience. *Frontiers in Neuroinformatics* **9**:11. doi:10.3389/fninf.2015.00011
Muller L, Chavane F, Reynolds J, Sejnowski TJ. 2018. Cortical travelling waves: Mechanisms and computational principles. *Nature Reviews Neuroscience* **19**:255–268. doi:10.1038/nrn.2018.20
Nandy A, Nassi JJ, Jadi MP, Reynolds J. 2019. Optogenetically induced low-frequency correlations impair perception. *eLife* **8**. doi:10.7554/eLife.35123
Nason SR, Vaskov AK, Willsey MS, Welle EJ, An H, Vu PP, Bullard AJ, Nu CS, Kao JC, Shenoy KV, Jang T, Kim H-S, Blaauw D, Patil PG, Chestek CA. 2020. A low-power band of neuronal spiking activity dominated by local single units improves the performance of brain–machine interfaces. *Nature Biomedical Engineering 2020* 1–11. doi:10.1038/s41551-020-0591-0
Němec P, Osten P. 2020. The evolution of brain structure captured in stereotyped cell count and cell type distributions. *Current Opinion in Neurobiology*, Neurobiology of Behavior **60**:176–183. doi:10.1016/j.conb.2019.12.005
Newman JP, Fong MF, Millard DC, Whitmire CJ, Stanley GB, Potter SM. 2015. Optogenetic feedback control of neural activity. *eLife*. doi:10.7554/eLife.07192
Oby ER, Golub MD, Hennig JA, Degenhart AD, Tyler-Kabara EC, Yu BM, Chase SM, Batista AP. 2019. New neural activity patterns emerge with long-term learning. *Proceedings of the National Academy of Sciences* **116**:15210–15215. doi:10.1073/pnas.1820296116
Ohta Y, Guinto MC, Tokuda T, Kawahara M, Haruta M, Takehara H, Tashiro H, Sasagawa K, Onoe H, Yamaguchi R, Koshimizu Y, Isa K, Isa T, Kobayashi K, Akay YM, Akay M, Ohta J. 2021. Micro-LED Array-Based Photo-Stimulation Devices for Optogenetics in Rat and Macaque Monkey Brains. *IEEE Access* **9**:127937–127949. doi:10.1109/ACCESS.2021.3111666
Packer AM, Roska B, Häuser M. 2013. Targeting neurons and photons for optogenetics. *Nature Neuroscience* **16**:805–815. doi:10.1038/nn.3427
Packer AM, Russell LE, Dalgleish HWP, Häusser M. 2015. Simultaneous all-optical manipulation and recording of neural circuit activity with cellular resolution in vivo. *Nat Methods* **12**:140–146. doi:10.1038/nmeth.3217
Pandarinath C, O'Shea DJ, Collins J, Jozefowicz R, Stavisky SD, Kao JC, Trautmann EM, Kaufman MT, Ryu SI, Hochberg LR, Henderson JM, Shenoy KV, Abbott LF, Sussillo D. 2018. Inferring single-trial neural population dynamics using sequential auto-encoders. *Nature Methods* **15**:805–815. doi:10.1038/s41592-018-0109-9
Parasuram H, Nair B, D'Angelo E, Hines M, Naldi G, Diwakar S. 2016. Computational modeling of single neuron extracellular electric potentials and network local field potentials using LFPsim. *Frontiers in Computational Neuroscience* **10**:65. doi:10.3389/fncom.2016.00065
Pearl J. 2009. Causality. New York: Cambridge University Press. doi:10.1017/CBO9780511803161
Peixoto D, Verhein JR, Kiani R, Kao JC, Nuyujukian P, Chandrasekaran C, Brown J, Fong S, Ryu SI, Shenoy KV, Newsome WT. 2021. Decoding and perturbing decision states in

real time. *Nature* **591**:604–609. doi:10.1038/s41586-020-03181-9

Peng Y, Mittermaier FX, Planert H, Schneider UC, Alle H, Geiger JRP. 2019. High-throughput microcircuit analysis of individual human brains through next-generation multineuron patch-clamp. *eLife* **8**:e48178. doi:10.7554/eLife.48178

Pettersen KH, Lindén H, Dale AM, Einevoll GT. 2012. Extracellular spikes and CSD. *Handbook of neural activity measurement* **1**:92–135.

Potter SM, El Hady A, Fetz EE. 2014. Closed-loop neuroscience and neuroengineering. *Frontiers in Neural Circuits* **0**:115. doi:10.3389/FNCIR.2014.00115

Prinz AA, Abbott LF, Marder E. 2004. The dynamic clamp comes of age. *Trends in Neurosciences* **27**:218–224. doi:10.1016/j.tins.2004.02.004

Prsa M, Galiñanes GL, Huber D. 2017. Rapid Integration of Artificial Sensory Feedback during Operant Conditioning of Motor Cortex Neurons. *Neuron* **93**:929–939.e6. doi:10.1016/j.neuron.2017.01.023

Rackauckas C, Nie Q. 2017. DifferentialEquations.jl – A Performant and Feature-Rich Ecosystem for Solving Differential Equations in Julia. *Journal of Open Research Software* **5**:15. doi:10.5334/jors.151

Rajalingham R, Piccato A, Jazayeri M. 2022. Recurrent neural networks with explicit representation of dynamic latent variables can mimic behavioral patterns in a physical inference task. *Nat Commun* **13**:1–15. doi:10.1038/s41467-022-33581-6

Ronzitti E, Conti R, Zampini V, Tanese D, Foust AJ, Klapoetke N, Boyden ES, Papagiakoumou E, Emiliani V. 2017. Submillisecond Optogenetic Control of Neuronal Firing with Two-Photon Holographic Photoactivation of Chronos. *J Neurosci* **37**:10679–10689. doi:10.1523/JNEUROSCI.1246-17.2017

Roth BL. 2016. DREADDs for Neuroscientists. *Neuron* **89**:683–694. doi:10.1016/j.neuron.2016.01.040

Rule ME, Vargas-Irwin C, Donoghue JP, Truccolo W. 2018. Phase reorganization leads to transient -LFP spatial wave patterns in motor cortex during steady-state movement preparation. *Journal of Neurophysiology* **119**:2212–2228. doi:10.1152/jn.00525.2017

Saleem AB, Lien AD, Krumin M, Haider B, Rosón MR, Ayaz A, Reinhold K, Busse L, Carandini M, Harris KD, Carandini M. 2017. Subcortical Source and Modulation of the Narrowband Gamma Oscillation in Mouse Visual Cortex. *Neuron* **93**:315–322. doi:10.1016/j.neuron.2016.12.028

Sani OG, Abbaspourazad H, Wong YT, Pesaran B, Shanechi MM. 2021a. Modeling behaviorally relevant neural dynamics enabled by preferential subspace identification. *Nature Neuroscience* **24**:140–149. doi:10.1038/s41593-020-00733-0

Sani OG, Pesaran B, Shanechi MM, Hsieh M. 2021b. Where is all the nonlinearity: flexible nonlinear modeling of behaviorally relevant neural dynamics using recurrent neural networks. *bioRxiv* 2021.09.03.458628. doi:10.1101/2021.09.03.458628

Sani OG, Yang Y, Lee MB, Dawes HE, Chang EF, Shanechi MM. 2018. Mood variations decoded from multi-site intracranial human brain activity. *Nat Biotechnol* **36**:954–961. doi:10.1038/nbt.4200

Santhanam G, Yu BM, Gilja V, Ryu SI, Afshar A, Sahani M, Shenoy KV. 2009. Factor-Analysis Methods for Higher-Performance Neural Prostheses. *Journal of Neurophysiology* **102**:1315–1330. doi:10.1152/jn.00097.2009

Saran S, Gupta N, Roy S. 2018. Theoretical analysis of low-power fast optogenetic control of firing of Chronos-expressing neurons. *Neurophotonics* **5**:1. doi:10.1117/1.nph.5.2.025009

Sato TK, Nauhaus I, Carandini M. 2012. Traveling Waves in Visual Cortex. *Neuron* **75**:218–229. doi:10.1016/j.neuron.2012.06.029

Scheffer LK, Xu CS, Januszewski M, Lu Z, Takemura S, Hayworth KJ, Huang GB, Shinomiya K, Maitlin-Shepard J, Berg S, Clements J, Hubbard PM, Katz WT, Umayam L, Zhao T, Ackerman D, Blakely T, Bogovic J, Dolafi T, Kainmueller D, Kawase T, Khairy KA, Leavitt L, Li PH, Lindsey L, Neubarth N, Olbris DJ, Otsuna H, Trautman ET, Ito M, Bates AS, Goldammer J, Wolff T, Svirskas R, Schlegel P, Neace E, Knecht CJ, Alvarado CX, Bailey DA, Ballinger S, Borycz JA, Canino BS, Cheatham N, Cook M, Dreher M, Duclos O, Eubanks B, Fairbanks K, Finley S, Forknall N, Francis A, Hopkins GP, Joyce EM, Kim S, Kirk NA, Kovalyak J, Lauchie SA, Lohff A, Maldonado C, Manley EA, McLin S, Mooney C, Ndama M, Ogundeyi O, Okeoma N, Ordish C, Padilla N, Patrick CM, Paterson T, Phillips EE, Phillips EM, Rampally N, Ribeiro C, Robertson MK, Rymer JT, Ryan SM, Sammons M, Scott AK, Scott AL, Shinomiya A, Smith C, Smith K, Smith NL, Sobeski MA, Suleiman A, Swift J, Takemura S, Talebi I, Tarnogorska D, Tenshaw E, Tokhi T, Walsh JJ, Yang T, Horne JA, Li F, Parekh R, Rivlin PK, Jayaraman V, Costa M, Jefferis GS, Ito K, Saalfeld S, George R, Meinertzhagen IA, Rubin GM, Hess HF, Jain V, Plaza SM. 2020. A connectome and analysis of the adult Drosophila central brain. *eLife* **9**:e57443. doi:10.7554/eLife.57443

Schneider S, Lee JH, Mathis MW. 2022. Learnable latent embeddings for joint behavioral and neural analysis. doi:10.48550/arXiv.2204.00673

Sharp AA, O'Neil MB, Abbott LF, Marder E. 1993. The dynamic clamp: artificial conductances in biological neurons. *Trends in Neurosciences* **16**:389–394. doi:10.1016/0166-2236(93)90004-6

Shenoy KV, Kao JC. 2021. Measurement, manipulation and modeling of brain-wide neural population dynamics. *Nature Communications* **12**:1–5. doi:10.1038/s41467-020-20371-1

Shenoy KV, Sahani M, Churchland MM. 2013. Cortical Control of Arm Movements: A Dynamical Systems Perspective. *Annu Rev Neurosci* **36**:337–359. doi:10.1146/annurev-neuro-062111-150509

Siegle JH, López AC, Patel YA, Abramov K, Ohayon S, Voigts J. 2017. Open Ephys: an open-source, plugin-based platform for multichannel electrophysiology. *J Neural Eng* **14**:045003. doi:10.1088/1741-2552/aa5eea

Smith JTH, Linderman SW, Sussillo D. 2021. Reverse engineering recurrent neural networks with Jacobian switching linear dynamical systemsAdvances in Neural Information Processing Systems. pp. 16700–16713.

Sporns O. 2018. Graph theory methods: applications in brain networks. *Dialogues in Clinical Neuroscience* **20**:111–121. doi:10.31887/DCNS.2018.20.2/osporns

Sridharan S, Gajowa MA, Ogando MB, Jagadisan UK, Abdeladim L, Sadahiro M, Bounds HA, Hendricks WD, Turney TS, Tayler I, Gopakumar K, Oldenburg IA, Brohawn SG, Adesnik H. 2022. High-performance microbial opsins for spatially and temporally precise perturbations of large neuronal networks. *Neuron* **110**:1139–1155.e6. doi:10.1016/j.neuron.2022.01.008

Srinivasan SS, Maimon BE, Diaz M, Song H, Herr HM. 2018. Closed-loop functional optogenetic stimulation. *Nature Communications* **9**:1–10. doi:10.1038/s41467-018-07721-w

Steinmetz NA, Aydin C, Lebedeva A, Okun M, Pachitariu M, Bauza M, Beau M, Bhagat J, Böhm C, Broux M, Chen S, Colonell J, Gardner RJ, Karsh B, Kloosterman F, Kostadinov D, Mora-Lopez C, O'Callaghan J, Park J, Putzeys J, Sauerbrei B, van Daal RJJ, Vollan AZ, Wang S, Welkenhuysen M, Ye Z, Dudman JT, Dutta B, Hantman AW, Harris KD, Lee AK, Moser EI, O'Keefe J, Renart A, Svoboda K, Häusser M, Haesler S, Carandini M, Harris TD. 2021. Neuropixels 2.0: A miniaturized high-density probe for stable, long-term brain recordings. *Science* **372**. doi:10.1126/science.abf4588

Stimberg M, Brette R, Goodman DFM. 2019. Brian 2, an intuitive and efficient neural simulator. *eLife* **8**. doi:10.7554/eLife.47314

Sussillo D. 2014. Neural circuits as computational dynamical systems. *Current Opinion in Neurobiology*, Theoretical and computational neuroscience **25**:156–163. doi:10.1016/j.conb.2014.01.008

Sussillo D, Barak O. 2013. Opening the Black Box: Low-Dimensional Dynamics in High-Dimensional Recurrent Neural Networks. *Neural Computation* **25**:626–649. doi:10.1162/NECO_a_00409

Svoboda K, Yasuda R. 2006. Principles of Two-Photon Excitation Microscopy and Its Applications to Neuroscience. *Neuron* **50**:823–839. doi:10.1016/j.neuron.2006.05.019

Tafazoli S, MacDowell CJ, Che Z, Letai KC, Steinhardt CR, Buschman TJ. 2020. Learning to control the brain through adaptive closed-loop patterned stimulation. *J Neural Eng* **17**:056007. doi:10.1088/1741-2552/abb860

Tal I, Neymotin S, Bickel S, Lakatos P, Schroeder CE. 2020. Oscillatory Bursting as a Mechanism for Temporal Coupling and Information Coding. *Frontiers in Computational Neuroscience* **14**.

Telenczuk B, Telenczuk M, Destexhe A. 2020. A kernel-based method to calculate local field potentials from networks of spiking neurons. *Journal of Neuroscience Methods* **344**:108871. doi:10.1016/j.jneumeth.2020.108871

Thornton C, Hutchings F, Kaiser M. 2019. The virtual electrode recording tool for extracellular potentials (VERTEX) Version 2.0: Modelling in vitro electrical stimulation of brain tissue. *Wellcome Open Research* **4**. doi:10.12688/wellcomeopenres.15058.1

Tomsett RJ, Ainsworth M, Thiele A, Sanayei M, Chen X, Gieselmann MA, Whittington MA, Cunningham MO, Kaiser M. 2015. Virtual Electrode Recording Tool for EXtracellular potentials (VERTEX): comparing multi-electrode recordings from simulated and biological mammalian cortical tissue. *Brain Structure and Function* **220**:2333–2353. doi:10.1007/s00429-014-0793-x

Vaidya AR, Pujara MS, Petrides M, Murray EA, Fellows LK. 2019. Lesion Studies in Contemporary Neuroscience. *Trends in Cognitive Sciences* **23**:653–671. doi:10.1016/j.tics.2019.05.009

Vierock J, Rodriguez-Rozada S, Dieter A, Pieper F, Sims R, Tenedini F, Bergs ACF, Bendifallah I, Zhou F, Zeitzschel N, Ahlbeck J, Augustin S, Sauter K, Papagiakoumou E, Gottschalk A, Soba P, Emiliani V, Engel AK, Hegemann P, Wiegert JS. 2021. BiPOLES is an optogenetic tool developed for bidirectional dual-color control of neurons. *Nature*

Communications **12**:1–20. doi:10.1038/s41467-021-24759-5

Vyas S, Golub MD, Sussillo D, Shenoy KV. 2020. Computation through Neural Population Dynamics. *Annual Review of Neuroscience* **43**:249–275. doi:10.1146/annurev-neuro-092619-094115

Wang G, Wyskiel DR, Yang W, Wang Y, Milbern LC, Lalanne T, Jiang X, Shen Y, Sun QQ, Zhu JJ. 2015. An optogenetics- and imaging-assisted simultaneous multiple patch-clamp recording system for decoding complex neural circuits. *Nature Protocols* **10**:397–412. doi:10.1038/nprot.2015.019

Wang L, Huang K, Zhong C, Wang L, Lu Y. 2018. Fabrication and modification of implantable optrode arrays for in vivo optogenetic applications. *Biophys Rep* **4**:82–93. doi:10.1007/s41048-018-0052-4

Wang Y, Boyd S. 2010. Fast Model Predictive Control Using Online Optimization. *IEEE TRANSACTIONS ON CONTROL SYSTEMS TECHNOLOGY* **18**:267. doi:10.1109/TCST.2009.2017934

Welkenhuysen M, Hoffman L, Luo Z, De Proft A, Van den Haute C, Baekelandt V, Debyser Z, Gielen G, Puers R, Braeken D. 2016. An integrated multi-electrode-optrode array for in vitro optogenetics. *Sci Rep* **6**:20353. doi:10.1038/srep20353

Wiegert JS, Mahn M, Prigge M, Printz Y, Yizhar O. 2017. Silencing Neurons: Tools, Applications, and Experimental Constraints. *Neuron* **95**:504–529. doi:10.1016/j.neuron.2017.06.050

Willett FR, Avansino DT, Hochberg LR, Henderson JM, Shenoy KV. 2021. High-performance brain-to-text communication via handwriting. *Nature* **593**:249–254. doi:10.1038/s41586-021-03506-2

Wilmes KA, Clopath C. 2019. Inhibitory microcircuits for top-down plasticity of sensory representations. *Nat Commun* **10**:5055. doi:10.1038/s41467-019-12972-2

Witt A, Palmigiano A, Neef A, El Hady A, Wolf F, Battaglia D. 2013. Controlling the oscillation phase through precisely timed closed-loop optogenetic stimulation: a computational study. *Frontiers in Neural Circuits* **7**:1–17. doi:10.3389/fncir.2013.00049

Wu J, Liang Y, Chen S, Hsu CL, Chavarha M, Evans SW, Shi D, Lin MZ, Tsia KK, Ji N. 2020. Kilohertz two-photon fluorescence microscopy imaging of neural activity in vivo. *Nature Methods* **17**:287–290. doi:10.1038/s41592-020-0762-7

Yang GR, Joglekar MR, Song HF, Newsome WT, Wang X-J. 2019. Task representations in neural networks trained to perform many cognitive tasks. *Nat Neurosci* **22**:297–306. doi:10.1038/s41593-018-0310-2

Yang Y, Qiao S, Sani OG, Sedillo JI, Ferrentino B, Pesaran B, Shanechi MM. 2021. Modelling and prediction of the dynamic responses of large-scale brain networks during direct electrical stimulation. *Nature Biomedical Engineering* **5**:324–345. doi:10.1038/s41551-020-00666-w

Zeng H. 2022. What is a cell type and how to define it? *Cell* **185**:2739–2755. doi:10.1016/j.cell.2022.06.031

Zenke F, Vogels TP. 2021. The Remarkable Robustness of Surrogate Gradient Learning for Instilling Complex Function in Spiking Neural Networks. *Neural Computation* **33**:899–925. doi:10.1162/neco_a_01367

Zhang L, Lee J, Rozell C, Singer AC. 2019. Sub-second dynamics of theta-gamma coupling in

hippocampal CA1. *eLife* **8**. doi:10.7554/eLife.44320

Zhang Z, Russell LE, Packer AM, Gauld OM, Häusser M. 2018. Closed-loop all-optical interrogation of neural circuits in vivo. *Nature Methods* **15**:1037–1040. doi:10.1038/s41592-018-0183-z